Feasibility Study of an EWICON System using the Self Adjusting Multinozzle Electrospraying Technique

Arjan Winters

September 5, 2011

Supervisor: Dr. ir. D. Djairam

Thesis committee

Prof. dr. J.J. Smit

Dr. ir. P.H.F. Morshuis

Dr. ir. D. Djairam

Dr. ir. J.C.M. Marijnissen

Delft University of Technology

Author: Arjan Winters

Student number:1144286

Department of High Voltage Technology and Asset Management

Faculty of Electrical Engineering, Mathematics and Computer Science

Delft University of Technology

Preface

During my master of electrical engineering I chose the specialization of high voltage systems and components. I became increasingly interested in renewable and sustainable energy, which resulted in an internship project in Kenya. Here, I explored the possibilities of sustainable energy applications on schools. I realized that sustainable energy would be the future and hopefully also my future. My supervisor, Peter Morshuis, suggested that the EWICON would be an interesting subject. The combination of sustainable energy and high voltage engineering seemed to be the perfect challenge to finalize my study. In an EWICON system, high voltage is applied to create charged droplets. Those droplets have to be displaced by the wind, thereby work is done and an increased potential energy can be obtained. In this way, wind energy is directly converted into electrical energy.

This thesis is the result of many experiments in the basement of the high voltage laboratory. Because this is a relatively new principle, much research had to be conducted to understand the processes involved during the conversion. During my research, it appeared that many factors were affecting stable and predictable measurements. To indicate the challenge of this research I would like to quote Lawrence Peter "Yogi" Berra: "In theory, there is no difference between theory and practice. But, in practice, there is." After adapting the setup several times, using simulation programs for the electric field distribution as well the airflow, I was able to generate electrical power directly from the wind.

I spent much time on my own, doing experiments, computer simulation and writing. Nevertheless, many people have, directly or indirectly, contributed to successfully obtain the results presented in this thesis.

First of all, I would like to thank my supervisor Dr. ir. Djairam for guiding me through this research. Secondly, I would like to acknowledge Prof. Smit and Dr. ir. Marijnissen for reviewing my work and being part of my thesis committee. I would also like to thank Dr.ir. Yurteri for helping me understand the complicated nature of electrospraying as well as Dr. ir. Morshuis for his advice.

I am very grateful for the assistance of the staff of the high voltage laboratory. Whenever my setup had to be adapted, or parts had to be fabricated, Wim Termorshuizen was more than willing to help me. Paul van Nes assisted me in carrying out the high voltage experiments. I would like to thank him for the confidence he had in me to do the experiments on my own and for sharing his expertise. The high voltage laboratory was a very comfortable learning environment, thanks to the expertise of the staff and fellow students but also thanks to the less serious conversations during tea-break.

Apart from technical advice, personal support was very important to me during my graduation project. Therefore, I would like to thank my fellow students, my roommates and friends. A special thanks will go to my parents and grandparents. They made it possible for me to study and always stimulated me to learn as much as possible. Last but not least, I would like to thank my girlfriend for her unconditional support. Even during your summer holiday you spent a lot of time with me and always encouraged me to achieve my goals. Thank you!

Abstract

This thesis describes the research which have been conducted on the self adjusting multinozzle electrospraying technique, applied in an electrostatic wind energy converter (EWICON). An EWICON system directly converts wind energy to electrical energy by the displacement of charged droplets in the opposite direction of an electric field. Electrospraying referrers to a process where nozzles are formed by so called Taylor cones. These cones form the nozzles which spray an aerosol of charged droplets. The self adjusting technique offers advantages compared to other methods with respect to electrospraying properties and utilization of material. For practical implementation, the following components have been simulated and tested.

First the electrode configuration was optimized for electrospraying. This configuration exists of two cylindrical conductors at a distance of 42 mm and a diameter ratio of 1 to 8. This ratio appeared to be able to generate the desired electric field for stable electrospraying while minimizing the velocity in which the charged droplets are attracted back to the system. A wind shield was designed and applied to locally increase wind speed and provide stable Taylor cone formation.

Secondly the creation of charged droplets was examined with this setup. A mixture of 30% ethanol and 70% demineralized water appeared to be the most suitable spraying liquid. Experiments were conducted to observe the relation between the flow rate and applied potential and the number of Taylor cones with the coresponding current. From these experiments can be concluded that it is desirable to generate a large number of Taylor cones while maintaining an as low as possible flow rate and charging potential. Higher potential will result in unstable spraying and corona discharges. It was discovered that the number of cones could be significantly be increased by making use of the hysteresis effect.

Finally the charging system was placed on an insulated self-supplying platform to complete the EWICON system. Experiments have been conducted, using a wind generator, to assess the performance according to output power. Results were compared to a similar needle configuration (using needles as nozzles) investigated by D. Djairam. There has been a significant improvement according to previous charging experiments with the self adjusting multinozzle system. However, the system efficiency is low compared to the needle system, due to the inability of removing all charged droplets from the system by the wind. A comparable output power could be achieved, when all charged droplets would be removed and improvements are realized according to the output power per nozzle. In this stage of this research, the advantages of the self adjusting character of the systems are being outweighed by the sensitivity to variations in flow rate, wind speed and electric field distribution. Another important aspect is the humidity of the surrounding air which causes leakage currents and disturbing the electrospraying process. In general, it can be concluded that the self adjusting multinozzle system offers perspective for implementation in an EWICON system. However, further research should be conducted to improve electrical, as well as aerodynamic performance.

Samenvatting

Deze scriptie beschrijft een haalbaarheids onderzoek naar een zichzelf instellende electrospraying methode met meervoudige sproeiers, toegepast in een electrostatic wind energy converter(EWICON). Een EWICON systeem is in staat om wind energie direct om te zetten in elektrische energie, door de wind elektrisch geladen druppels tegen de richting van een elektrisch veld te laten bewegen. Electrospraying is een methode om geladen druppeltjes te creëren doormiddel van een elektrisch veld. Zogenaamde Taylor cones vormen de sproeiers, welke een fijne mist van geladen druppeltjes verspreidt. De zelf instellende methode biedt in principe voordelen ten opzichte van andere toegepaste technieken met betrekking tot eigenschappen van electrospraying en materiaalgebruik. Voor een praktische toepassing zijn de volgende onderdelen gesimuleerd en getest.

Ten eerste is er een elektrode configuratie ontworpen en geoptimaliseerd voor electrospraying. Deze configuratie bestaat uit twee cilindrische geleiders met een diameter verhouding van 1 op 8. Deze verhouding is optimaal gebleken in de balans tussen de concentratie van het elektrisch veld op de gewenste locatie en het reduceren van de snelheid waarmee de geladen druppels worden terug getrokken naar het systeem. Een windscherm is ontworpen met als functie de Taylor cones te beschermen tegen de wind alsmede lokaal de windsnelheid te vergroten.

Vervolgens is er met deze opstelling onderzoek verricht naar het proces waarbij geladen druppeltjes worden gegenereerd. Een mix, bestaande uit 30% ethanol en 70% gedistilleed water, bleek de meest geschikte sproeivloeistof. Verschillende experimenten zijn uitgevoerd om het verband te onderzoeken tussen de spanning en debiet en het aantal Taylor cones met de bijbehorende elektrische stroom. Het is wenselijk om zoveel mogelijk Taylor cones te creëren terwijl de spanning en debiet zo laag mogelijk blijven. Hoge waarden van de spanning resulteren in instabiele electrospraying en corona ontladingen. Door gebruik te maken van het hysterese effect, kan het aantal Taylor cones aanzienlijk verhoogd worden terwijl er aan boven genoemde voorwaarden wordt voldaan.

Als laatste is het oplaadsysteem op een zelf voorzienend, geïsoleerd platform geplaatst om het EWICON systeem compleet te maken. Dit platform wordt opgeladen als de geladen druppels worden afgevoerd door de wind. Het opgeleverde vermogen is vergeleken met een andere methode (waarbij naadjes de sproeiers vormen), onderzocht door Dr.ir. Djairam, om de werking van het zichzelf instellende systeem te toetsen. Hoewel er een aanzienlijke vooruitgang is geboekt met betrekking tot het succesvol opladen van het platform, is het geleverde vermogen slechts een fractie van het vergelijkbare naalden systeem. De oorzaak hiervan is, dat niet alle geladen druppels verplaatst worden door de wind. Mocht dit wel het geval zijn, én er verbeteringen zijn gerealiseerd ten opzichte van het geproduceerde vermogen per sproeier, zal het mogelijk zijn om vergelijkbare resultaten te verkrijgen.

In deze fase van het onderzoek weegt het voordeel van het zichzelf instellende vermogen van deze techniek nog niet op tegen de nadelen. Namelijk, de gevoeligheid voor verstoringen door zowel de ongelijkmatigheid van het systeem zelf als invloeden van buitenaf. De luchtvochtigheid speelt een belangrijke rol bij de prestaties van het systeem. Een hoge luchtvochtigheid resulteert in lekstromen en verstoring van het electrospraying proces. Er kan geconcludeerd worden dat de zichzelf instellende electrospraying techniek perspectief biedt voor de implementatie in een EWICON systeem. Verder onderzoek zal gedaan moeten worden om zowel de elektrische als aerodynamische prestaties te verbeteren.

Contents

1. Introduction **1**
- 1.1. Wind as an energy resource . . . 1
- 1.2. Conventional wind energy conversion . . . 2
  - 1.2.1. General design . . . 2
  - 1.2.2. Betz' law . . . 3
- 1.3. Wind turbine versus EWICON system . . . 4
- 1.4. Self adjusting multinozzle system . . . 5
- 1.5. Research objectives . . . 5
- 1.6. Experimental approach . . . 6
- 1.7. Scope . . . 6
- 1.8. Thesis outline . . . 6

2. EWICON working principle **9**
- 2.1. Principle . . . 9
- 2.2. Forces on charged droplets . . . 10
- 2.3. Practical implementation . . . 11
  - 2.3.1. System components . . . 12
  - 2.3.2. EWICON system types . . . 12
- 2.4. Conclusions . . . 13

3. Charged droplet creation methods **15**
- 3.1. Charged droplet creation . . . 15
  - 3.1.1. Rayleigh limit . . . 15
  - 3.1.2. Charge to mass ratio . . . 15
  - 3.1.3. Electrical mobility . . . 16
  - 3.1.4. High pressure monodisperse spraying . . . 17
  - 3.1.5. Electrohydrodynamic atomization . . . 17
- 3.2. Electrospraying modes . . . 19
- 3.3. Cone jet mode . . . 20
- 3.4. Droplet size and current . . . 20
- 3.5. Electric field . . . 22
- 3.6. Self adjusting multinozzle system . . . 23
- 3.7. Conclusions . . . 24

4. Electrode configuration **25**
- 4.1. Experimental setup . . . 25
- 4.2. Electrode configuration . . . 25
  - 4.2.1. Electric field distribution. . . . 26
  - 4.2.2. Airflow . . . 30
- 4.3. Power density . . . 32
- 4.4. Conclusion . . . 32

5. Electrospraying experiments **35**
- 5.1. Requirements . . . 35
- 5.2. Experiments . . . 35
  - 5.2.1. Number of cones and flow rate . . . 35
  - 5.2.2. Hysteresis effect . . . 36
  - 5.2.3. Onset potential . . . 39

5.2.4. Polarity 40
5.3. Factors affecting stable electrospraying 41
5.3.1. Humidity 41
5.3.2. Liquid flow 41
5.3.3. Electric field 41
5.4. Conclusions 42

6. Complete EWICON system **43**
6.1. Hypotheses 43
6.2. Setup 43
6.2.1. Test procedure 44
6.3. Experiments 45
6.3.1. Flow rate 46
6.3.2. Charging potential 46
6.3.3. Number of cones 46
6.3.4. Wind speed 48
6.4. System efficiency 49
6.5. Conclusions 50

7. Conclusions and recommendations **51**
7.1. Conclusions per chapter 51
7.2. General conclusions 52
7.3. Recommendations 52

A. Spraying liquid properties **57**

B. Software tools **59**
B.1. Solidworks 59
B.2. Lorentz 59

C. Electric field; theory and simulation **61**

D. Humidity **63**

E. Experimental setup **65**

Nomenclature **69**

References **72**

1. Introduction

Energy is one of the most important aspects of modern life. Without energy, transport, communication or production of goods will not be possible. More than 80 percent of the energy consumption in the world is produced by combustion of fossil fuels [1]. Due to global warming and depletion of those fossil fuels, a substitution by alternative energy resources will be inevitable. The safety of one of those alternatives, nuclear fission, was challenged during the aftermath of the earthquake in Japan, March 2011. Renewable energy seems to be the only solution to maintain the current standard of living, without compromising the needs of future generations. Renewable energy resources are regenerating or natural energy flows, like wind energy. In paragraph 1.1, an overview will be given of the history of wind energy, followed by the conventional method to convert wind energy into electrical energy in paragraph 1.2. Section 1.3 compares wind turbines with a new concept, the EWICON system. A new technique which could be applied in an EWICON system, will be described in 1.4. This technique will be the main subject for this research. The research objectives are stated in section 1.5, followed by the experimental approach, scope and the outline of this thesis in paragraph 1.6 to 1.8 respectively.

1.1. Wind as an energy resource

Wind energy has been used for more than 7000 years, as boats were propelled by the wind on the Nile river in Egypt at 5000 B.C. The first recording of windmill design dates from 500-900 A.D, however, the first documentation of a windmill originates from China at 1219 B.C. These mills, had a vertical rotating axis and were made of wood and reed sails. They were used for grinding and water pumping (figure 1a). The first European windmills had a horizontal axis configuration and from the 13th to the 18th century the Dutch refined this design with the tower mill (figure 1b). The blades could be moved into the direction of the wind and because of the crankshaft the applications became more versatile like sawing and making paper, however, they are well known for draining lakes. In the 18th century, the steam engine took over the mechanical work, and the number of windmills declined. In 1888, Charles F. Brush invented the first electrical wind turbine, which had a rotor diameter of 17 meter and a electrical output power of 12kW (figure 1c).

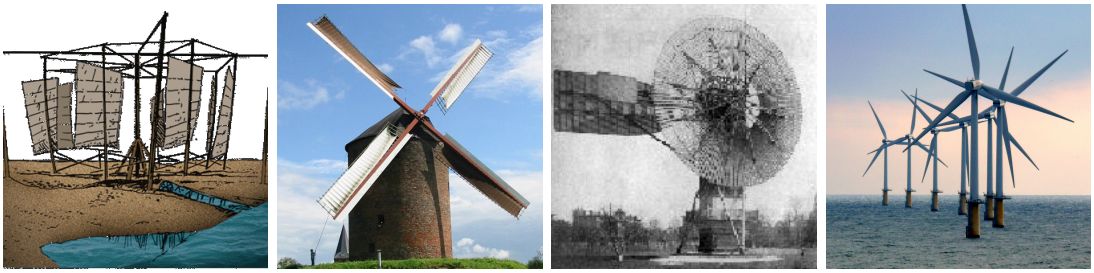

(a) (b) (c) (d)

Figure 1: Development of windmills: (a) First documented design of a Persian windmill (b)A Dutch tower mill (c) The first electrical wind turbine (d) Prinses Amalia wind farm, 120 MW offshore wind warm in The Netherlands.

In the 20th century, wind turbine design benefits from government programs and aerospace development. The applications vary from a few kilowatts rural electric-

ity supply to multi-megawatt grid connected wind farms, both onshore as offshore (figure 1d). In 2009 wind energy contributed for 2.1 percent to the total electricity production (see figure 2). However, while this percentage is rather small, wind energy is the fastest growing renewable resource as shown in figure 3.

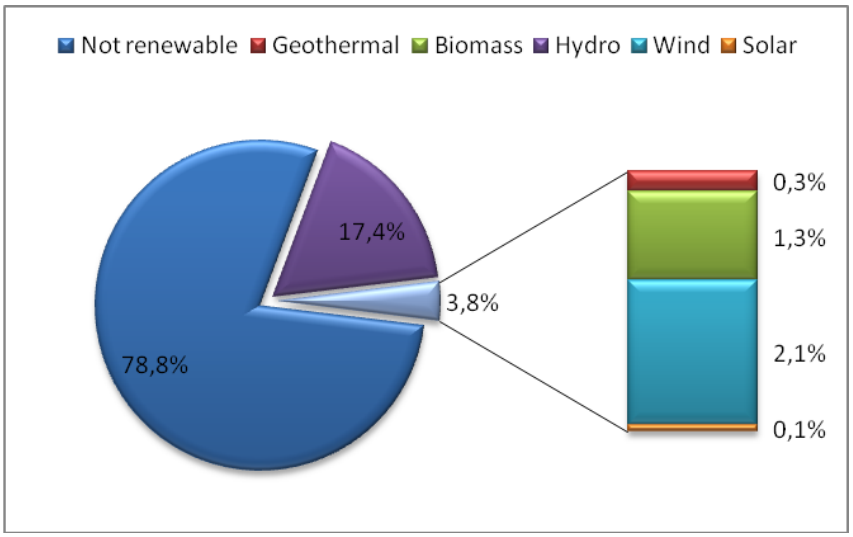

Figure 2: Worldwide electricity generation 2009 [3]. Wind energy provides 2.1% of the electricity generation in the world.

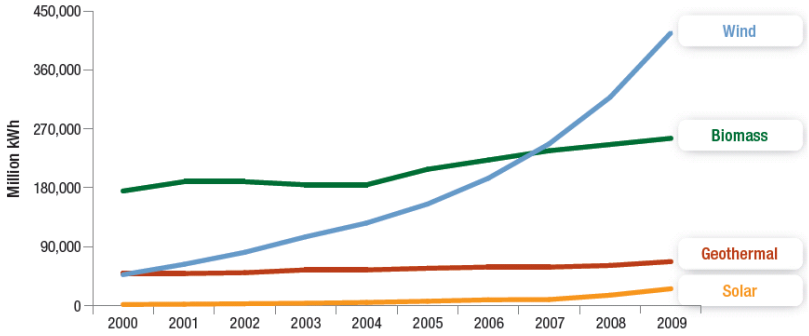

Figure 3: Renewable Electricity Generation Worldwide by Technology [2]. Wind energy is the fastest growing renewable energy source.

1.2. Conventional wind energy conversion

1.2.1. General design

The design of a wind turbine has been largely improved since the early windmills. Materials have become stronger and lightweight. Aerodynamic design and conversion to electrical energy have become more efficient resulting in a 7.5 MW wind turbine with a rotor diameter of 126 meters. At the moment, the E126 by Enercon is worlds largest wind turbine. Despite technological developments, the basic concept i.e. the energy of the wind is converted to rotational energy, did not change.

In a conventional wind energy converter, or wind turbine, the blades (typically 3) transform the kinetic wind energy into rotational energy. A gearbox which connects

the rotor to the generator accelerates the relatively slow rotation. The generator transforms the rotational energy into electrical energy. These components are placed inside a nacelle which is mounted to a tower. A controller keeps the nacelle in the direction of the wind and the blades in optimal position. All parts are schematically depicted in figure 4a. A typical power curve of a wind turbine is illustrated in figure 4b. The cut-in speed, is the minimum required wind speed (about 3.5 m/s) at which the turbine is able to efficiently generate electrical power. From the cut-in speed, the power increases with wind speed up to the rated power of the wind turbine. At higher wind speeds the pitch of the blades is adjusted, which decreases efficiency but enables the wind turbine to produce electricity at the rated power. At the cut-out speed (above 25 m/s), the mechanical forces become to large for safe operation and the wind turbine is shut down.

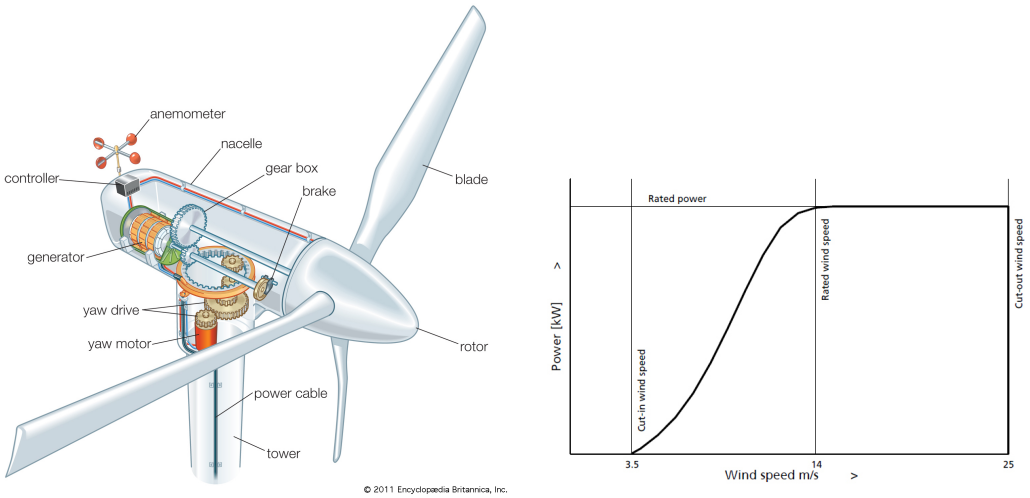

(a) Components of a common wind turbine with a gearbox .

(b) Typical power curve for a wind turbine.

Figure 4: Conventional wind energy conversion. The wind energy is converted into rotational energy which enables a generator to produce electrical power.

This example gives an impression of the most common wind turbine design namely a horizontal axis wind turbine with a gearbox. Other designs are, for example, direct drive wind turbines, where the generator is directly coupled to the rotor, or vertical axis wind turbines.

1.2.2. Betz' law

A theoretical maximum efficiency exists at which wind energy can be converted into useful mechanical energy. This limit is given by Betz' law [4]. The power of the wind is given by

$$P_w = \frac{1}{2} \cdot A \cdot \rho_a \cdot v_w^3 \tag{1}$$

where A is the surface area, ρ_a is the density of air and v_w the velocity of the wind. There is an optimal ratio between the wind speed before and after the converter. The speed after the converter should be $\frac{1}{3}$ of the initial wind speed to extract the maximum power. The maximum recoverable power, (P_{max}) of a wind energy converter is given by

$$P_{max} = \frac{8}{27} \cdot A \cdot \rho_a \cdot v_w^3 \tag{2}$$

Combining formula 1 and 2 results in the upper limit of the efficiency of a wind energy converter.

$$\frac{P_{max}}{P_w} = \frac{16}{27} \approx 59\% \tag{3}$$

This limit applies to every conversion method, including the new concept to be described in this thesis; the EWICON system. This means that, even before knowing the specific workings, there is no gain in maximum efficiency using the EWICON system with respect to conventional energy conversion.

1.3. Wind turbine versus EWICON system

One of the disadvantages of the mechanical conversion method is the wear and tear of the moving parts. Therefore, these components are more subjective to failure and have high maintenance costs. Another drawback is the noise and intermittent shadow caused by the rotational movement of the blades. Also visual pollution of the landscape is mentioned as a negative property of a wind turbine.

A new concept, which converts the wind energy directly into electrical energy, is the Electrostatic WInd energy CONverter or EWICON. The EWICON directly converts wind energy into electrical energy, by displacement of charged particles by the wind in the opposite direction of an electric field. With this method the moving mechanical part, and its disadvantages, is no longer present. Another advantage is, that the size of this converter i.e. the wind surface area, can be scaled in two directions. In a conventional converter this area can only be increased by increasing the rotor diameter, see figure 5.

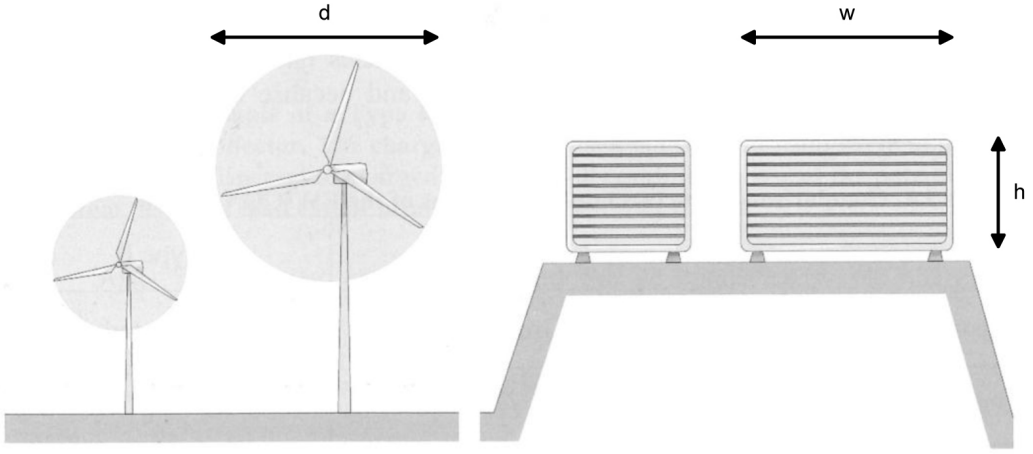

Figure 5: Wind surface area of both wind energy converters. At a wind turbine, the area is increased by increasing the rotor diameter (d). An EWICON system can be scaled up by increasing the height (h) or the width (w), or both.

The principle of the EWICON system is the work done by the wind on a charged particle when it is displaced in an electric field. This results in an increase of potential electrical energy. An electrical load can be connected to the system and the

energy can be used. The working principle will be extensively discussed in chapter 2. Summarizing, the advantages of the EWICON system are:

- No mechanical wear and tear, thereby lower maintenance costs
- No intermittent shadows and lower noise because the absence moving and rotating parts
- Area can be increased in both dimensions

Despite the advantages, there will be also some restrictions by implementing an EWICON system. The charged particles will be represented by charged droplets. As a consequence, a liquid will be released in the environment, which has to be environmentally friendly. Also corrosion, and clogging of the liquid supply should be taken into account.

However the EWICON system can be scaled in two dimensions, the size will still be in the order of a conventional wind turbine. The visual pollution problem will not be solved. The complete system as well as the creation of charged droplets operates at high voltage, as will be explained in chapter 4. This requires attention to safety and insulation aspects.

1.4. Self adjusting multinozzle system

The concept of the EWICON system has been proven to successfully convert wind energy into electrical energy, using water. Research has been conducted by Dr. ir. Djairam on different types of EWICON systems according to charged droplet creation methods and general design [5]. On a very small scale, a positive output power was generated, by displacing charged droplets with a wind generator.

Different methods and configurations exist to create these charged droplets, which will be discussed in chapter 3. A specific method, namely electrohydrodynamic atomization, is of interest. This technique has the potential to create a simple and cheap, large scale EWICON system. It has been observed that, after rain, charged droplets sprayed from high voltage lines. This technique could be implemented in a EWICON system. A wire shaped electrode is put on a high potential while a liquid is distributed on the surface. Charged droplets originate from various nozzles along the electrode. Those nozzles appeared to be self adjusting, both in number and size, due to applied potential and liquid flow rate.

1.5. Research objectives

The goal of this thesis is to investigate the feasibility of a large scale EWICON system, using the self adjusting multinozzle technique, described in the previous paragraph. To achieve this goal, the following issues have to be examined:

- Theoretical analysis of electrospraying process and parameters influencing the creation of charged droplets
- Construction of a charging system with respect to electric field distribution and airflow
- Investigate relation between system input parameters and expected output power
- Combine results to test a complete EWICON system.

1.6. Experimental approach

The concept of an EWICON system is relatively new and still in an early stage of development. Hence, a considerable amount of experiments has to be conducted to realize the goals described before. Firstly, a theoretical basis will be established to predict the parameters which exist when a charged droplet is created and affected by an electric field. Subsequently, an experimental setup has to be constructed, based on computer simulations of the electric field distribution and airflow. Various configurations have to be tested and the best performing setup will be used for further experimentation. Once the charged droplet creation method and corresponding setup are obtained, experiments have to be conducted to investigate how the input parameters affects the output of the system. A relation has to be obtained between flow rate and applied potential with respect to the number of spraying nozzles and output current. With those results the system could be tuned to generate maximum power at varying wind speed. Finally, a complete EWICON setup will be created to verify the expected results and judge whether or not the self adjusting multinozzle system would be feasible for a large scale EWICON system.

1.7. Scope

Ultimately, the EWICON system should be able to replace conventional wind turbines, generating clean and renewable energy. In this thesis, the main focus is on the development and performance of a small scale self adjusting system. In other words, a stable and predictable output when certain input conditions are given. There are many factors influencing the performance of the EWICON system, which fall beyond the scope of this research. The most important issue is the application of tap or saline water, using this particular charged droplet creation technique.

1.8. Thesis outline

In chapter 2, the basic principle will be explained; work is done by the force of the wind on a charge droplet, present in an electric field. All forces which act on such a droplet will be described. Different configurations will be given to use this technique to create an electrostatic wind energy converter.

Chapter 3 gives an overview of charged droplet creation methods. Limitations on maximum charge and size will be presented. One specific charging method, electrospraying, will be explained in more detail since this method will be used in the experiments. Equations will be presented to predict the current and size per droplet as well the required electric field to obtain electrospraying.

Chapter 4 will be dedicated to the experimental setup with the emphasis on the electrode configuration. The effect on the electric field distribution as well the airflow will be investigated, varying the electrode size and shape. Both experiments and computer simulations will be used to obtain the optimal electrode configuration for further research.

In chapter 5, the relation between liquid flow rate, applied potential and output current will be analyzed. Experiments are conducted with the setup from chapter 4 and results will be compared with the equations from chapter 3. With these results it will be possible to adapt the system input parameters to obtain maximum power density at a given wind speed.

A complete EWICON system will be presented in chapter 6. The knowledge obtained about the optimal setup and the input parameters will be verified. As the system is charged by a wind generator, the output power will be compared to the input power to determine the efficiency. The complete system will be compared with a similar configuration.

Finally in chapter 7, conclusions about the performance of a self adjusting multi-nozzle system will be presented. The feasibility of this technique for an EWICON system will be discussed together with recommendations for further research.

2. EWICON working principle

In this chapter, the working principle of an EWICON system will be explained. In 2.1, the general principle will be described. The work that is done on charged particles, which is caused by the various electrical and mechanical forces, results in an electric potential rise of the system. In 2.2, all forces which act on a single charged droplet will be discussed. The practical implementation can be done with two possible configurations to convert the wind into electrical energy, as showed in 2.3. In section 2.4 conclusions will be given about the used system type.

2.1. Principle

The principle of the EWICON system is the work on a charged particle that is done by an electric force due to an electric field. The force ($\vec{F}$) on a particle with charge (q) in an electric field (E) is given by

$$\vec{F} = q \cdot \vec{E} \tag{4}$$

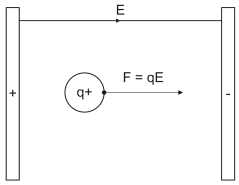

Figure 6: Force as a result of a charge in an electric field. In an EWICON system, the charge will be represented by a charged droplet.

The work (W) done on this particle is defined by the displacement (x) of this force given by

$$W = \vec{F} \cdot \vec{x} \tag{5}$$

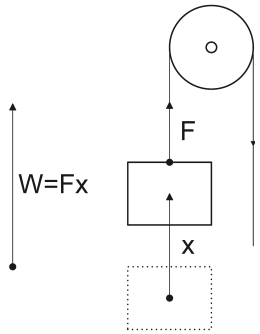

Figure 7: Work is done by the displacement of a force. In an EWICON system, the wind will be responsible for the displacement of the force on the charged droplet.

The force consists of a mechanical and an electrical component caused by the wind an the electric field respectively. Each component has a magnitude and a direction. If the force of the wind is in the opposite direction and larger than the electric force, the electrical potential energy of the charged particle will increase. It is comparable

with lifting a mass against gravity, when a mass is moved in the opposite direction of force field, its potential energy (U) increases.

$$dW = -dU \tag{6}$$

In an EWICON system, the charged particle is represented by a charged droplet. An applied voltage creates the electric field. As the wind removes the charged droplets from the system, the potential electrical energy rises. Two possible methods to use this potential electrical energy will be described in paragraph 2.3.

2.2. Forces on charged droplets

Different forces act on a charged droplet when present in an electric field, as depicted in figure 8. Mechanical forces are caused by the wind, gravity and buoyancy. Electrical forces originate from the external electric field and the charge present on surrounding droplets.

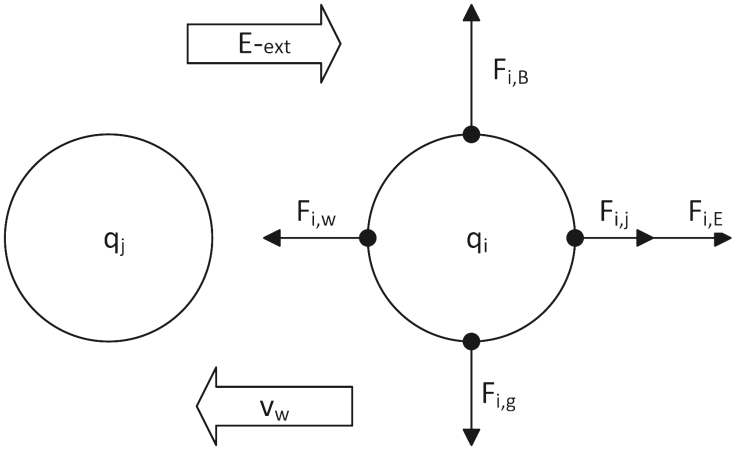

Figure 8: Forces which act on two charged droplets. Electrical forces exist due to an applied potential difference and the influence of the charge on each droplet. Mechanical forces are formed by gravity and wind.

From the work that is done on a single droplet, the potential energy difference can be calculated. The total energy produced by the wind can be calculated by taking the sum of all charged droplets. The work done on an arbitrary droplet i , is given by formula 7.

$$W_i = \int \left(\vec{F}_i - \vec{F}_{i,w}\right) \cdot \overrightarrow{dl} \tag{7}$$

where dl is the trajectory of the droplet, $\vec{F}_{i,w}$ the drag force of the wind acting on this droplet given by formula 8. $\vec{F}_i$ is the sum of all forces acting on this droplet given by formula 9 and visualized in figure 8. In the equation of $\vec{F}_{i,w}$, it is assumed that the flow process is laminar.

$$\vec{F}_{i,w} = \frac{3\pi \cdot \eta_a \cdot d_i \left(\vec{v}_w - \vec{v}_d\right)}{C_c} \tag{8}$$

where η_a is the dynamic absolute viscosity of air, d the droplet diameter, $\vec{v}_w$ the wind speed, $\vec{v}_d$ the speed of the droplet and C_c is the correction factor of Cunningham which is assumed to be 1 for particles larger than 1 μm.

$$\vec{F}_i = \vec{F}_{i,g} + \vec{F}_{i,B} + \vec{F}_{i,w} + \vec{F}_{i,E} + \sum \vec{F}_{i,j} = m_i \cdot \vec{a}_i \tag{9}$$

The mechanical forces are the gravity force and the buoyancy given by formula 10 and 11 respectively.

$$\vec{F}_{i,g} = m_i \cdot \vec{g} \tag{10}$$

in which m_i is the mass of this droplet and g the gravity constant.

$$\vec{F}_{i,B} = -\rho_a \cdot V_d \cdot \vec{g} \tag{11}$$

where ρ_a is the density of air and V_d the volume of the droplet. The electrical forces are given by the external electric field and the charge of the surrounding droplets given by formula 12 and 13 respectively.

$$\vec{F}_{i,E} = q_i \cdot \vec{E}_{ext} \tag{12}$$

in which q_i is the charge present on the droplet and E_{ext} the external electric field.

$$\vec{F}_{i,j} = \frac{1}{4\pi\varepsilon_0} \cdot \frac{q_i \cdot q_j}{r_{i,j}^2} \cdot r_{i,j} \tag{13}$$

where ε_0 is the dielectric constant of vacuum and $r_{i,j}$ the distance between droplet i and j. To give an impression of the order of magnitude, each force has been calculated and presented in table 1. This calculation is based on the a droplet which consists of 30% ethanol and 70% water. The droplet diameter is 10 μm and maximum charge is applied. The wind speed is 6 m/s and the external electric field 10^5 V/m. From table 1 can be concluded that the dominant forces are generated by the wind and the external electric field.

Table 1: Calculated forces on a single charged droplet for a 10 μm and maximum charged droplet, in an electric field of 10^5 V/m . The wind speed is 6 m/s. The dominant forces are $\vec{F}_{i,E}$ and $\vec{F}_{i,w}$.

Force component	Value [N]
$\vec{F}_{i,w}$	$1.0 \cdot 10^{-8}$
$\vec{F}_{i,g}$	$4.9 \cdot 10^{-12}$
$\vec{F}_{i,B}$	$6.2 \cdot 10^{-15}$
$\vec{F}_{i,E}$	$1.5 \cdot 10^{-8}$
$\vec{F}_{i,j}$	$2.1 \cdot 10^{-11}$

2.3. Practical implementation

In the previous section, the principle has been explained to generate a potential rise from the displacement of charge droplets. An electric field is required, as well as charge carrier. The force of the wind will have to displace this charge and the system should be able to rise in potential electrical energy.

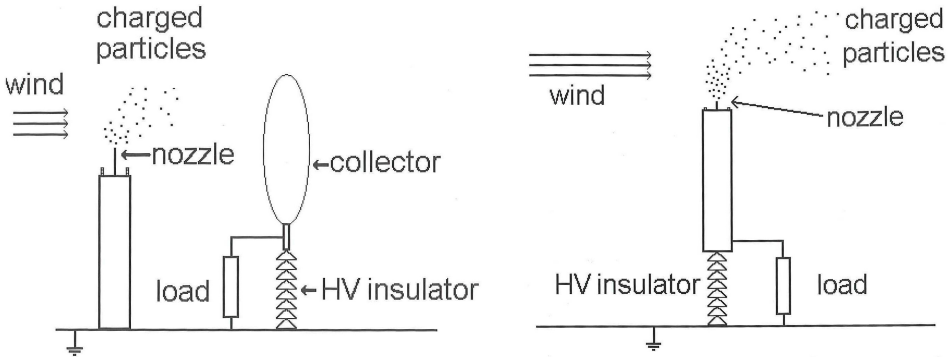

Figure 9: Two different EWICON system types [5]. (a) EWICON system where an insulated collector captures the charged particles. (b) The EWICON system itself is insulated and the earth functions as a charge collector.

2.3.1. System components

The following components are required for an EWICON system to successfully harvest energy from the wind.

- Liquid supply and charged droplet creation
- Generation of electric field
- Interaction with the wind and displacement of charged droplets

Since the liquid is the charge carrier, it has to be supplied and distributed to the system in a controlled and accurate way. This should require as little energy as possible to improve the system efficiency. Subsequently, the liquid has to be transformed into small charged droplets. Different methods, to acquire such droplets will be extensively explained in chapter 3.

Once charged droplets have been created, the electric field will generate the force on the charged droplets. This electric field is formed due to an applied potential between two electrodes. In chapter 4, different configurations will be examined.

Displacement of the charged droplets, by the force of the wind, will ultimately increase the potential energy of the complete system. Two possible configurations exist to achieve this.

2.3.2. EWICON system types

The first option is, to capture the charged particles with an insulated collector. As it collects charge, its potential rises and when an electrical load is attached, the stored charge can be used. This will be referred to, as a type A system.

The system itself can also be insulated from earth. Here, the complete system potential rises as the earth acts as a charge collector. This is the case with the type B EWICON. The stored charge can be used when an electrical load is connected to the system. Both types are illustrated in figure 9.

The disadvantage of type A is, that it requires an extra construction for the charge collector, which also complicates alignment with the wind. Type B is a single construction, however, the complete setup has to be insulated from earth. The

system has to be self supplying with respect to the power which will be required for the liquid pump and the high voltage source. Ultimately arrays of charging systems using sea water have to provide an amount of energy comparable to conventional wind turbines. An artists impression of such a system is depicted in figure 10.

2.4. Conclusions

In this chapter, the basic principle has been explained, which is the work done by the wind on a charged droplet in an electric field. To implement this principle into an EWICON system, charged droplets have to be created, an electric field has to be generated and the wind should be able to displace these charged droplets. Two system types were explained to utilize the removed charge. Type B will be used for further experiments. With this setup, the system will be insulated and the earth acts as a charge collector, resulting in a electrical potential rise of the system.

Figure 10: An artists impression of an offshore EWICON system. Ultimately, the EWICON will be able to replace offshore wind turbines.

3. Charged droplet creation methods

The efficient and controlled creation of charged droplets is essential for the operation of an EWICON system. In paragraph 3.1, different methods to create charged droplets will be discussed. One of these methods i.e. electrospraying, will be explained in more detail in 3.2 and 3.3, since it will be used for this research. Equations to calculate droplet size and produced current will be presented in 3.4. In paragraph 3.5 the influence of the electric field on electrospraying will be explained. The theory in this chapter will be used to verify the experiments in the next chapters.

3.1. Charged droplet creation

The energy conversion from wind energy to electrical energy, is done by the movement of charged droplets in an electric field. The creation of charged droplets can be done by several techniques. The most common methods are high pressure mono disperse spraying and electrohydrodynamic atomization. Both methods have been proven to be suitable for implementation in an EWICON system [5]. Before the different methods will be explained, the effects of a charge on a liquid will be discussed.

Hereafter, in every example or picture referring to droplets or a spraying liquid, a mixture of 30% ethanol and 70% demineralized water is meant. The motive for this particular liquid will be explained in paragraph 3.4 and the liquid properties used for calculation are given in appendix A.

3.1.1. Rayleigh limit

For every charging method, there is a limit to the amount of charge which can be present on a single droplet given by the Rayleigh limit (equation 14). If a droplet is charged, charge accumulates at the surface of this droplet. Because the charges have the same polarity, they repel each other. At a given moment the amount of charge results in an electric stress which is larger than the surface tension and the droplet breaks up into smaller droplets. Just before break-up, the Rayleigh limit is reached.

$$q_{max} = 8\pi\sqrt{\gamma \cdot \varepsilon_0 \cdot r_d^3} \tag{14}$$

where q_{max} is the Rayleigh charge limit, γ is the surface tension of the liquid, ε_0 is the dielectric constant of vacuum and r_d the droplet radius.

3.1.2. Charge to mass ratio

From the Rayleigh limit, it can be seen that the charge increases with droplet diameter, which implies that large droplets will be advantageous. However, if the charge is divided by the mass of that droplet, the relative charge or charge to mass ratio (CMR), increases with decreasing droplets size. This number indicates the produced charge per unit of time at a fixed liquid flow rate. The CMR can be calculated with

$$CMR = \frac{q}{m_{droplet}} \tag{15}$$

The CMR will be used to justify input parameters of the charged droplet production. An example is given in figure 11, where the CMR is given as a function of droplet size. According to the CMR, it seems to be favorable to have maximum charged droplets, as small as possible. In this way, at a fixed flow rate, the highest

amount of charge can be displaced by the wind per unit of time. However, another effect occurs when a charged droplet is present in an electric field, which has to be taken into account, namely the electrical mobility.

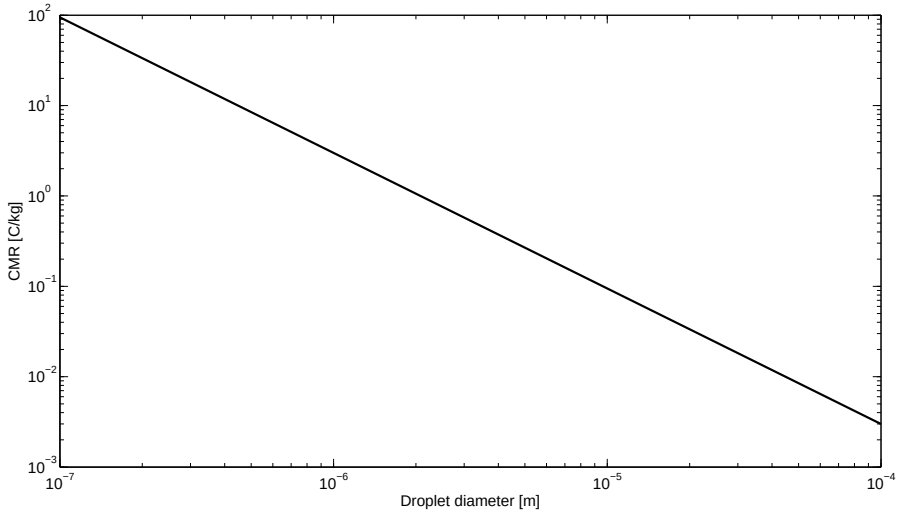

Figure 11: Charge to mass ratio as a function of droplet size. As the size of the droplets becomes smaller, the relative charge on the droplet increases.

3.1.3. Electrical mobility

When a charge is present in an electric field, a force causes this charge to move. The velocity in which a charge is able to move in an electric field is called the electrical mobility and is given by

$$\mu_e = \frac{v_T}{E} = q \cdot \mu_m \tag{16}$$

in which v_t is the terminal electrostatic velocity. The drag force of the wind results in the mechanical mobility (μ_m) given by

$$\mu_m = \frac{v_T}{F_w} \tag{17}$$

where F_w is the drag force of the wind given by formula 8. When equation 16, 17 and 8 are substituted, under the assumption that $\vec{v}_w - \vec{v}_d$ is equal to v_T, an equation can be derived to calculate v_T.

$$v_T = \frac{E \cdot q}{3 \cdot \pi \cdot \eta_a \cdot d} \tag{18}$$

In figure 12, the terminal electrostatic velocity is given as a function of electric field at different droplet sizes. The velocity of the wind has to be larger than v_T to transport the droplet away from the electric field. From this figure, two conclusions can be drawn:

- A high electric field results in high electrostatic velocity
- The terminal electrostatic velocity decreases as droplet size decreases

For example, to obtain a maximum terminal electrostatic velocity of 1 m/s, the droplet size should be smaller than 10 μm at a field strength of 10^4 V/m. If the droplet size is 100 μm, the field strength should be restricted to $3 \cdot 10^3$ V/m to obtain the same v_T.

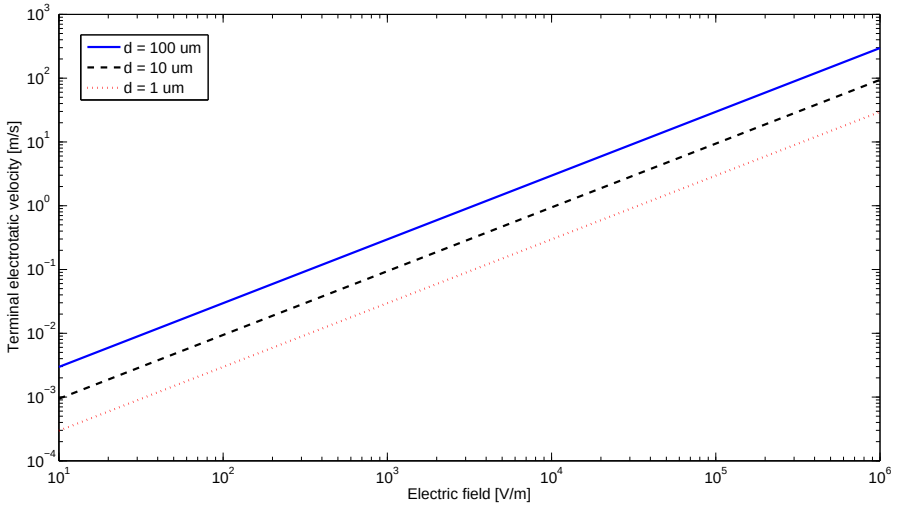

Figure 12: Terminal electrostatic velocity as a function of electric field at different droplet sizes. For successfully transporting charged droplets by the wind, the droplet size or the electric field should be restricted.

From the CMR and the electrical mobility, it can be concluded that the charging method should produce small droplet size and high droplet charge. Under the condition that the electric field in the direction of the wind should be limited.

3.1.4. High pressure monodisperse spraying

The first method to create small charged droplets is high pressure monodisperse spraying (HPMS). A jet is created by forcing a liquid at a high pressure through micron sized pores. This jet breaks up into monodisperse droplets which are being charged by external electrodes as depicted in figure 13a. This technique is applied in e.g. inkjet printers. Main advantage of HPMS is that the droplets are monodisperse and water or saline water can be used as spraying liquid. A drawback of HPMS is the relatively high energy needed to create charged droplets, which has a negative effect on the efficiency, when implemented in an EWICON system.

3.1.5. Electrohydrodynamic atomization

The second method is electrohydrodynamic atomization (EHDA) or electrospraying. This is a process where a liquid jet breaks up into an aerosol of charged droplets under the influence of an electric field. The creation and charging occurs simultaneously, requiring less energy as in HPMS. There are many applications which are making use of the small size of the droplets. In the biomedical industry, medication is solved in a liquid and is delivered in small quantities by electrospraying. EHDA is also used for the creation of micro- or nano-sized materials and coatings. In general, an EHDA setup consists of a a hollow conductive needle and a ground electrode perpendicular to this needle. A liquid is forced through the needle and a DC potential is applied

obtain EHDA, see figure 13b. There are different modes of EHDA depending on the surface tension and conductivity of the liquid and on the electric field strength as well the liquid flow rate. Properties of electrospraying will be discussed in more detail, since it appeared to be the most suitable method for this research.

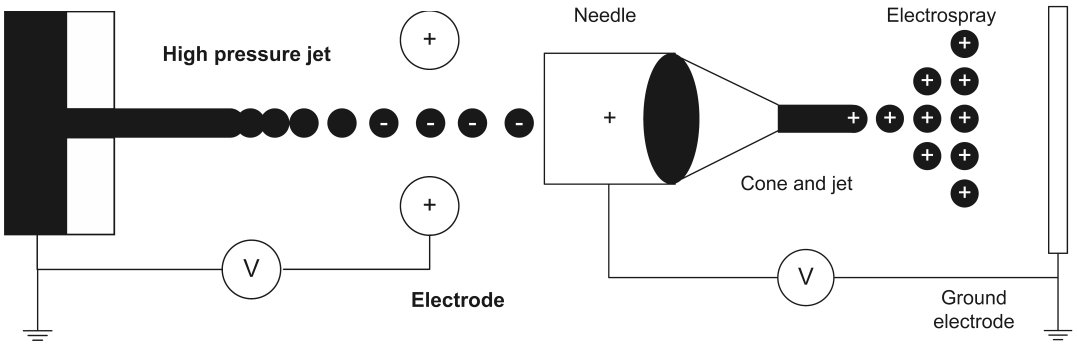

(a) HPMS (b) EHDA

Figure 13: Schematic representation of two methods to create small charged droplets. (a) High pressure monodisperse spraying. (b) Electrohydrodynamic atomization.

3.2. Electrospraying modes

When a DC potential is applied to an electrode which is in contact with the spraying liquid, the electric field interacts with the surface tension, transforming the shape of the droplet. As the potential is increased different electrospraying modes will be obtained, which are described below and depicted in figure 14.

a) Normal dripping; If no potential is applied, droplets will be released from the surface under the force of gravity

b) Fast dripping; Droplets are deformed and released at increased frequency

c) Intermittent cone jet mode; The droplet transforms into a cone shape and a thin jet emerges at the apex of the cone. This jet releases a droplet and the cone relaxes into its original shape.

d) Cone jet mode; The droplet is deformed into a stable cone and a thin jet emerges from the apex. This jet breaks up into an aerosol of small droplets

e) Cone jet mode; The cone size decreases as the potential is increased

f) Multi jet mode; Multiple cones originate from the same location

g) Negative cone; If a negative potential is applied, the spread of the aerosol is narrow compared to a positive potential

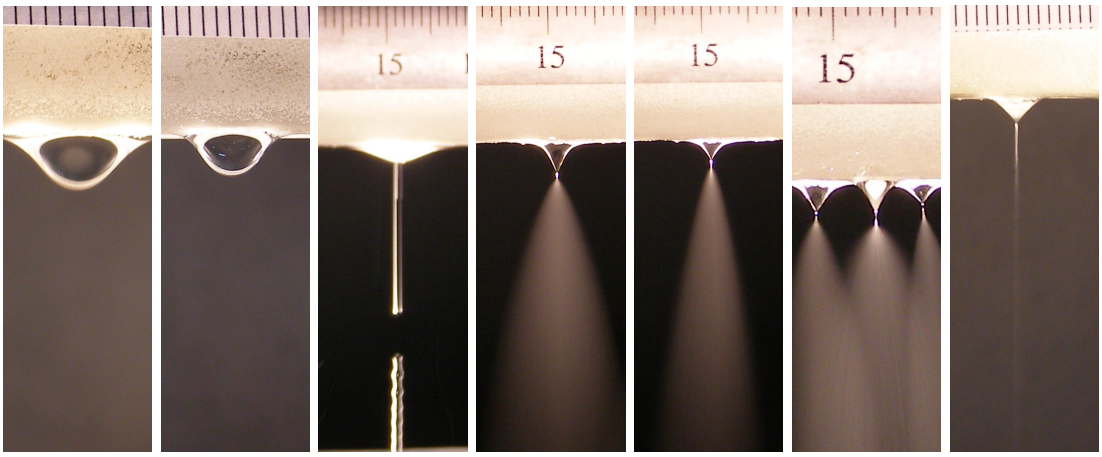

(a) (b) (c) (d) (e) (f) (g)

Figure 14: Different modes of EHDA; (a) No potential applied (b) 10kV, the droplet deforms. (c) 15kV, intermittent cone jet mode, a charged droplet is released. (d) 18kV, cone jet mode, an aerosol of charged droplets at the apex of the cone. (e) 26kV cone jet mode, the cone becomes smaller as the potential is increased. (f) 28 kV multiple jet mode. (g) -24 kV, Cone at negative applied potential.

Because the cone jet mode is stable and continuously produces small, monodisperse and highly charged droplets, this mode is preferable for experimentation. Small droplets will result in a high CMR and low v_T, which has been derived in the previous paragraph. Much research has been conducted to this specific mode, due to its wide range of applications. Droplet size and current can be calculated as will be explained in the next paragraphs.

3.3. Cone jet mode

Taylor (1964) was the first to describe the relation between the normal electric stress and the surface tension stress in a cone [20]. Electrospraying cones are therefore often referred as Taylor cones. Taylor cones form, when the electrical stress overcomes the surface tension stress of the spraying liquid. On the surface of the liquid, free surface charge, which consists of ions, is induced by the electric field. The tangential component of the electric field causes acceleration of the ions in the direction of the cone apex. The ions interact with the liquid resulting in a thin jet which emerges at the apex of the cone. This acceleration process and the shape of the cone are determined by a balance between gravity, electric stress at the surface, liquid pressure, and surface tension of the liquid. A schematic representation of a Taylor cone is given in figure 15. The jet breaks up into an aerosol of micrometer-size droplets which are highly charged due to a surplus of free surface charge. The droplets have the same polarity, therefore they repel each other and the aerosol spreads out as depicted in figure 14d. The cone jet mode is achieved when the above mentioned process, produces a continuous aerosol of charged droplets with a small size distribution.

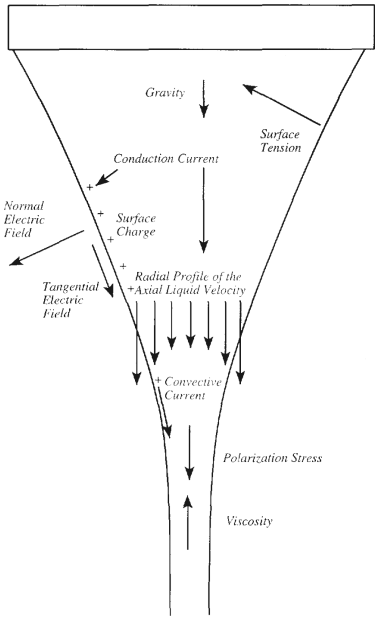

Figure 15: Schematic representation of a Taylor cone[6].

3.4. Droplet size and current

Under normal conditions, when no electric field is present, droplets are formed under the force of gravity. In case of a thin circular capillary, the droplet size is given by

$$d = \left(\frac{6 \cdot d_0 \cdot \gamma}{\rho \cdot g} \right)^{\frac{1}{3}} \tag{19}$$

where d_0 is the flow diameter of the capillary, γ is the surface tension and ρ the liquid density [13]. The order of magnitude is a few millimeters. Once the cone-jet mode is established the droplet diameter and current are determined by the properties of the spraying liquid and the flow rate. Different scaling laws for current and droplet size were found by de la Mora and Loscertales (1994) [22] and Gañán-Calvo et al (1997) [21]. To determine which law is valid a dimensionless number,

the viscosity number (VN), has been introduced. The viscosity number given by formula 20, gives the relation between the flow rate and the liquid properties which are defined by the viscosity, conductivity, and surface tension.

$$VN = \left(\frac{\gamma^3 \cdot \varepsilon_0^2}{\mu^3 \cdot K^2 \cdot Q} \right)^{\frac{1}{3}} \tag{20}$$

where μ is the dynamic viscosity, K is the conductivity and Q the flow rate. In this thesis, a simplified version of the scaling laws will be used, derived by Yurteri, Hartman and Marijnissen (2010) [7]. In case of a flat radial profile of the axial liquid velocity in the Taylor cone, the corresponding current (I^*) can be calculated with

$$I^* = 2.17 \cdot \sqrt{\gamma \cdot K \cdot Q} \tag{21}$$

Otherwise, when the radial profile is not flat, the actual current (I) can be determined with 22, which is valid for VN smaller than 10.

$$I = I^* \cdot (1 - 0.1 \cdot VN^{-0.45}) \tag{22}$$

For calculation of the droplets size, two equations are presented for two different breakup modes of the liquid jet, namely varicose and whipping breakup. Without going into detail it is assumed that the smallest size of equation 23 and 24 will be valid.

$$d_{varicose} = \left(\frac{16 \cdot \rho \cdot \varepsilon_0 \cdot Q^3}{\gamma \cdot K} \right)^{\frac{1}{6}} \tag{23}$$

$$d_{whipping} = \left(0.8 \cdot \frac{288 \cdot \varepsilon_0 \cdot \gamma \cdot Q^2}{I^2} \right)^{\frac{1}{3}} \tag{24}$$

For more information and derivation of the formulas used above the reader is referred to [7].

Figure 16 visualizes the influence of the fluid properties on the current, size and charge (as a percentage of the maximum charge given by the Rayleigh limit) per droplet. The equations above are applied to a mixture of demineralized water and ethanol at different flow rates. More information about the properties of the spraying liquid can be found in appendix A. From figure 16, the following relations can be formulated about the spraying liquid.

VN The viscosity number is low, so equation 21 can be used to calculate the current

Current The current increases with flow rate and decreases as the spraying liquid contains more ethanol

Size The droplet diameter increases with flow rate and ethanol percentage

Charge The charge increases with flow rate and decreases with ethanol percentage

CMR The CMR decreases with flow rate and ethanol percentage

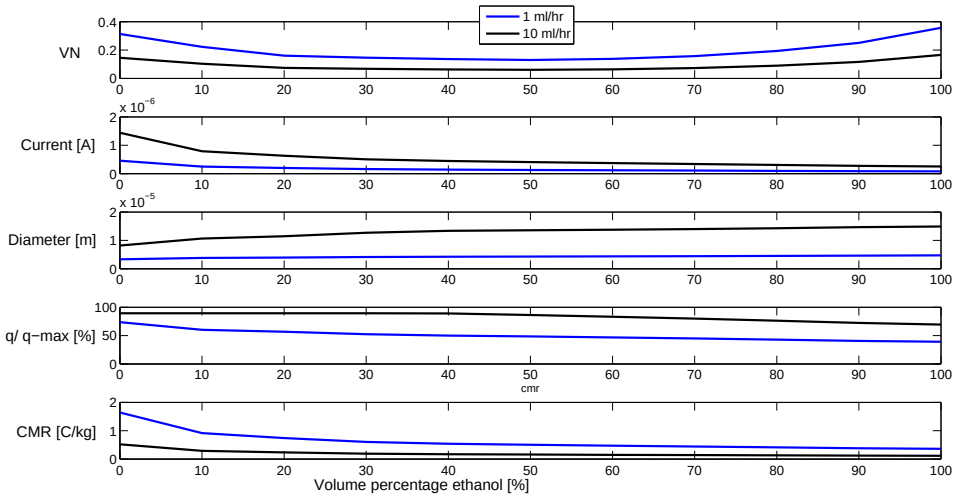

Figure 16: Calculated viscosity number, current, diameter and charge per droplet as a function of volume percentage ethanol mixed with water. From this figure can be concluded that the spraying liquid has to contain a low percentage of ethanol to increase charge per droplet. A high flow rate has a positive effect on the charge per droplet, but the increase in size has a negative effect on the CMR and electrical mobility.

From these relations can be concluded that the spraying liquid should contain as less ethanol as possible, however, as will be discussed in the next paragraph, the surface tension should be low to obtain stable EHDA. Experiments demonstrated that below 30% ethanol, no stable electrospraying was possible with the current test setup. The spraying liquid for further experimentation will consist of 30% ethanol and 70% demineralized water. The ethanol reduces the surface tension while the water contributes to a high output current and charge.

On one hand with respect to the charge, the flow rate should be high to achieve charging close to the Rayleigh limit. On the other hand, the size increases with flow rate which has a negative effect on the CMR. The size also influences the maximum allowable electric field with respect to the electrical mobility. For example, the electric field should not exceed 10^4 V/m or the flow rate should not exceed 10 ml/hr to keep v_T below 1 m/s.

The values in the graph are based on calculation, under the assumption that the liquid is spraying in the cone jet mode. Experiments have to point out if this mode could be achieved with a different setup as the needle-plate configuration.

3.5. Electric field

As mentioned before, the electric field determines in which mode the electrospraying process occurs. The value and shape of the electric field are determined by the applied potential and the electrode geometry. The required electric field is determined by the surface tension of the spraying liquid and the capillary radius. The onset electric field (the minimum required field to initiate electrospraying) E_0 is in the

order of 10^6 V/m [11, 14] and given by

$$E_0 = \sqrt{\frac{2 \cdot \gamma \cdot cos(\theta)}{\epsilon_0 \cdot r}} \tag{25}$$

where γ is the liquid surface tension, θ is the half angle of the cone and r the needle radius. In general the electric field is given by the potential V and a geometrical parameter $f(r, h)$ which is a function of the capillary radius and the distance between the electrodes.

$$E_0 = \frac{V}{f(r, h)} \tag{26}$$

For the needle setup the best approximation for the geometry is given by

$$f(r, h) = A \cdot r \cdot ln\left(\frac{4 \cdot h}{r}\right) \tag{27}$$

in which A is a constant from experimental data. When equations 25 to 27 are substituted the onset potential V_0 can be calculated.

$$V_0 = A \cdot \sqrt{\frac{2 \cdot \gamma \cdot r \cdot cos(\theta)}{\epsilon_0}} \cdot ln\left(\frac{4 \cdot h}{r}\right) \tag{28}$$

The surface tension of the spraying liquid is an important parameter whether or not electrospraying is possible. If the liquid has a high surface tension such as water, a high potential is required to initiate electrospraying, which leads to the risk of electrical breakdown of the surrounding air.

3.6. Self adjusting multinozzle system

Most research on EHDA has been conducted to single nozzle systems with conducting needles and a ground plate. Therefore the theory in this chapter is based on such a setup. For implementation in the EWICON system, a large amount of needles would be needed to scale up the system, which is impractical and costly.

It was discovered that Taylor cones were distributed along the conductor of high voltage lines during rain. This could be implemented in an EWICON system, by making a wire-shaped conductor together with a liquid supply. To expand the system, only a longer conductor and liquid channel would be required. The Taylor cones are free to move along the conductor. The number and size of these cones change with flow rate and applied potential. This could lead to another advantage, namely that this system adapts to wind speed. In this way the potential or flow rate can be tuned to obtain maximum power at every wind speed. To achieve such a system, firstly an electrode configuration and a liquid distribution has to be constructed. Secondly, research has to be conducted on the relation between the input parameters (electrode configuration, voltage and flow rate) and the output parameters (spraying in cone jet mode, number of Taylor cones, output current). Finally the optimized setup with corresponding parameters will be placed in a complete EWICON system, to convert the energy of the wind into electrical energy.

3.7. Conclusions

From this chapter can be concluded that small highly charged droplets are desirable. This will result in a high CMR, which means a high displacement of charged droplets will be possible per unit of time. This small size is also advantageous for the terminal electrostatic velocity. The speed in which droplets are attracted back to the electrode, reduces with decreasing droplet size.

The best option to create small charged droplets will be EHDA in the cone jet mode. The spraying liquid will be a mixture of 30% ethanol and 70% demineralized water. Calculations show that the droplets could be charged up to 90 percent of the Rayleigh limit and are in the order of a few micrometers. The size and charge of the droplets vary with flow rate. The flow rate should be kept low to obtain the highest CMR.

To achieve electrospraying, the electric field has to overcome the liquid surface tension. The local electric field should be in the order of 10^6 V/m. This could be realized, depending on the electrode geometry and the applied voltage which will be investigated in the next chapter.

A new technique has been introduced to create multiple Taylor cones, namely the self adjusting multinozzle system, which will be the core of this research. First the optimal electrode configuration has to be determined to create multiple electrospraying nozzles. Secondly, research will be conducted to verify if the cone-jet mode will be achieved and if the calculations in this chapter could be applied.

4. Electrode configuration

The components needed for an EWICON setup have been briefly discussed in section 2. These components will be discussed in detail in this chapter with the emphasis on the electrode configuration. Two electrodes will be required to create an electric field to initiate electrospraying. Firstly, a general experimental setup of a self adjusting multinozzle system is explained in section 4.1. The geometry determines the electric field distribution and the airflow. Both experiments and computer simulations will be used to obtain the optimal electrode configuration. In paragraph 4.2.1, the electrical properties will be examined while in paragraph 4.2.2, the focus is on the airflow around the setup. In section 4.3, the power density is given, which will be utilized for the experiments in the next chapter.

4.1. Experimental setup

The experimental setup [8] consists of two main components to generate charged droplets which are given by the liquid supply and the creation of an electric field. For an accurate and equally distributed liquid supply, a syringe pump (Harvard apparatus, PHD 2000 infusion) is used. This pump drives two syringes which are connected with tubes to a flow distributor consisting of eight nozzles which spread the liquid equally to the liquid channel. This liquid channel consists of a support structure and a strip of porous material (Porex) to create an uniform liquid film. A schematic representation is given in figure 17.

A high voltage (HV) power supply (Fug, HCN 35-65000), which is able to apply both positive and negative potential up to 65 kV DC. The HV-electrode is a wire-shaped conductor which is embedded inside the porous material. At a distance from the HV electrode, a ground-electrode is present to create an electric field. It appeared that the dimensions of the liquid channel with respect to the conductor are very sensitive. Thus, the creation of an uniform liquid film could be easily disturbed [8]. For this reason, the HV-electrode and liquid channel remain constant at the current setup. This means that the dimensions of the liquid channel and electrode as well the depth of the electrode into the porous material will not be changed. The distance and the shape of the ground electrode will be varied, to change the magnitude and distribution of the electric field.

4.2. Electrode configuration

The electrode configuration determines the geometry of the setup. It affects both the electrical properties as well the airflow between the electrodes. Firstly, the electric field distribution will be examined, using Lorentz. Lorentz is a computer simulation program based on the boundary element method. With this program, field plots can be generated of all electric field components to analyze the electric field distribution.

Secondly, the airflow will be simulated with FloXpress. With this a simulation tool in a CAD program called Solidworks, the airflow can be visualized. More information about the software tools can be found in appendix B

From the computer simulations and experiments, the best performing electrode configuration will be selected according to the performance of electrospraying and airflow.

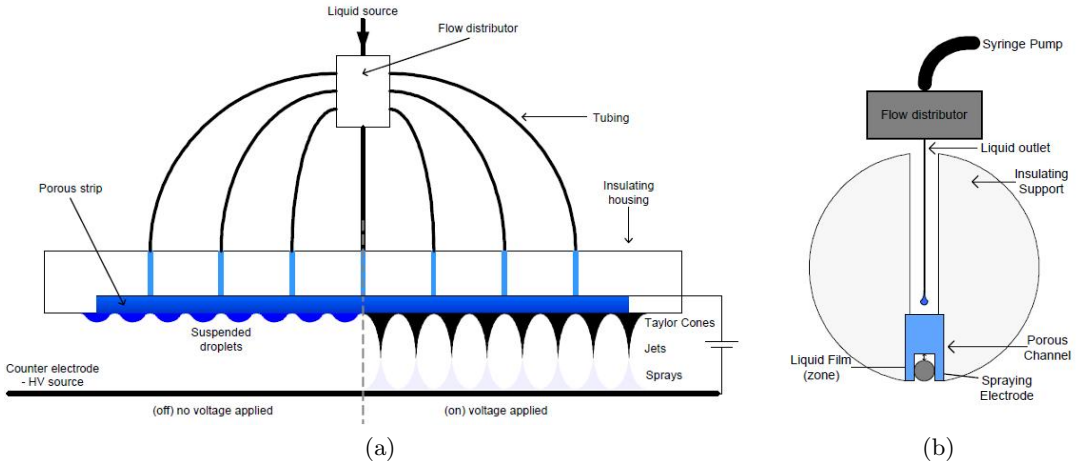

Figure 17: Experimental setup for a self adjusting multinozzle system, as investigated by A. Theodore [8]. (a) Front view including the spraying liquid, with and without applied potential. (b) Side view where the porous material with the embedded HV-electrode is visible.

4.2.1. Electric field distribution.

As discussed in section 3.5, the electric field is created by the applied potential and the electrode configuration. The potential determines the field strength while the geometry will be responsible for the electric field distribution. To simulate the needle-plate setup, the electric field should be concentrated at the HV-electrode. At the liquid channel, the field should be high (in the order of 10^6 V/m) to initiate electrospraying. Between the HV and ground-electrode, the field should decline to avoid breakdown of the surrounding air.

Different electrode shapes (see figure 18) were placed at various distances, to investigate the electrospraying process. The following effects were investigated.

- Successful electrospraying with a plate and a cylindrical electrode.
- Effect of remaining liquid on the surface with a solid and a mesh type of each electrode
- Successful electrospraying with different sizes of the cylindrical electrode.

The first two aspects appeared to have no influence on the electrospraying process. No difference was observed using a plate or cylindrical shape. Likewise, stable Taylor cones were formed regardless of the remaining liquid at the electrode surface.

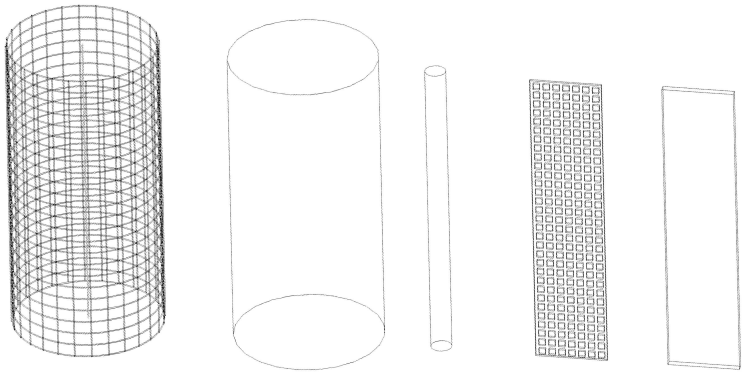

Figure 18: Different ground-electrode shapes. Each shape exists in a mesh and a solid type to investigate the influence of residual liquid and airflow. The size determines the electric field concentration at the HV-electrode.

The various sizes of the cylindrical electrodes determine the ratio of the ground-electrode to the HV-electrode. This ratio is given by

$$R = \frac{r_g}{r_{HV}} \tag{29}$$

in which r_g is the radius of the ground-electrode and r_{HV} the radius of the HV-electrode which is 1 mm. As this ratio becomes larger, the electric field concentrates more at the HV-electrode. In figure 19, the tangential component of the electric field is given for different values of R. This component determines whether or not electrospraying will occur. In figure 19, field plots of the tangential component of the electric field are presented at three different ground electrodes. As the size of the ground electrode and, therefore, R was decreased, the electric field concentration shifts from the HV- to the ground-electrode. This effect can also be observed in figure 20, which presents the value of the electric field is as a function of the distance from the HV-electrode to the surface of the ground-electrode. It appeared that, when R was decreased to a value lower than 8, the electric field at the HV-electrode was not sufficiently high to obtain stable electrospraying.

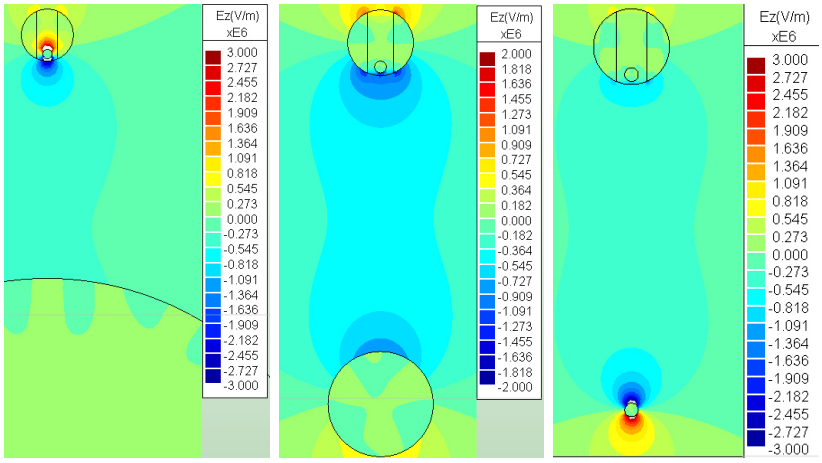

(a) R= 57.5 (b) R=8 (c) R=1

Figure 19: Field plots with different sized ground-electrodes. The potential and distance are constant at 23 kV and 42 mm respectively. When R decresases, the concentration of the electric field shifts from the HV-electrode to the ground electrode .

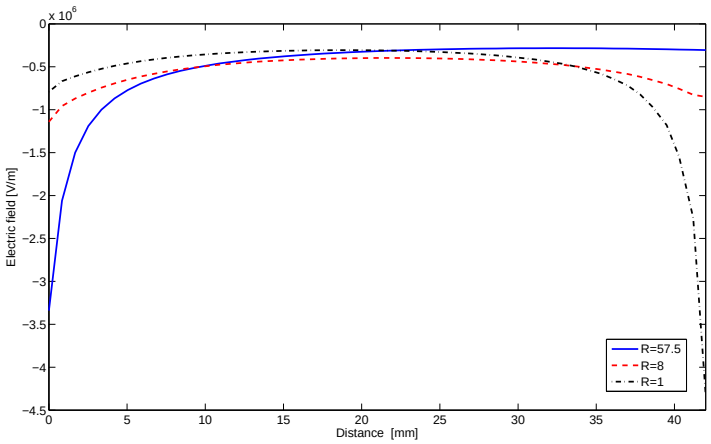

Figure 20: Value of the tangential electric field of the different electrode ratio as a function of distance from the HV-electrode. The concentration of the electric field shifts from the HV-electrode to the ground-electrode as R decreases.

The electrode ratio also effects the normal component of the electric field, which is in the opposite direction of the wind, depicted in figure 21. This component (E_{VT}) determines the terminal electrostatic velocity for a certain droplet size. As R increases, E_{VT} will rise as well. This can be observed in more detail in figure 22 where the value of E_{VT} is given as a function of the distance on a horizontal line, which originates at the center of the gap between the electrodes.

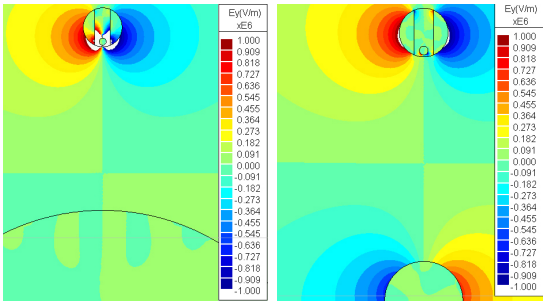

(a) R = 57.5 (b) R = 8

Figure 21: Component of the electric field in the opposite direction of the wind at different values of R. As R increases E_{VT} increases as well.

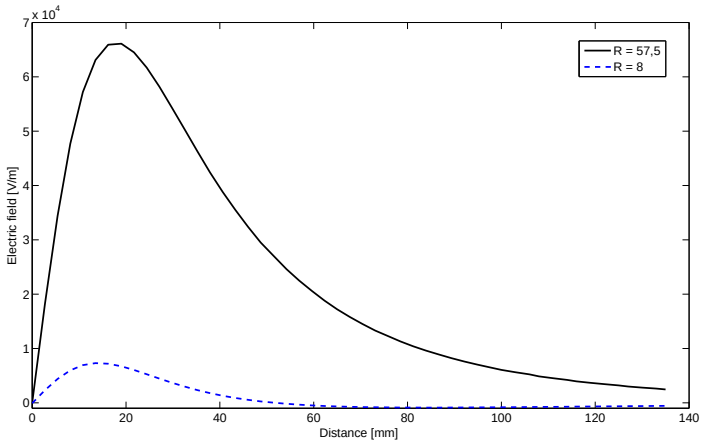

Figure 22: Value of E_{VT} at different values of R as a function of distance from the charging system. The disadvantage of a large R, is a high E_{VT}, thus a high terminal electrostatic velocity.

The maximum value of E_{VT} occurs at a distance of about 2 cm from the charging system. A large difference of E_{VT} at different ratio, can be observed in figure 22. The terminal electrostatic velocity is proportional to E_{VT}. Consequently, there will be a large difference of v_T between the two electrode configurations, as indicated in table 2. The effect on a maximum charged $10\mu m$ droplet is given calculated with equation 14 and 18.

Table 2: The terminal electrostatic velocity of a maximum charged, 10 μm droplet at different values of R and various distances.

R	v_T at 2 cm [m/s]	v_T at 4 cm [m/s]	v_T at 10 cm [m/s]
57.5	5.8	3.4	0.5
8	0.6	0.1	0

From figure 19, it can be concluded, that the increase in ratio between the electrodes has a positive effect on the tangential electric field which is favorable for electrospraying. At a value of R smaller than 8, no stable spraying was achieved.

The electric field in the opposite direction of the wind also increases with this ratio. On the contrary, this increase in ratio will have a negative effect on the terminal electrostatic velocity.

When the shape and size of the electrode are determined, the distance of the ground-electrode can be adjusted. The advantage of a larger distance between the electrodes, is the larger available area where the wind can act on the charged droplets. On the other hand the potential has to be increased as well to generate the required electric field. This results in possible corona discharges in the surrounding air.

4.2.2. Airflow

As mentioned before, the geometry of the setup also affects the airflow at he location of the charged droplets. The advantage of the cylindrical electrode with a large R, is that the velocity of the wind, in the gap between the electrodes, will be increased. This is simulated in FloXpress and confirmed by experiments. In figure 23, the airflow is given for the solid cylinder and the mesh cylinder at a wind speed of 6 m/s. Electrically, they perform equally, however, the wind speed is increased 1.5 times at the solid cylinder while at the mesh cylinder the wind speed is not affected.

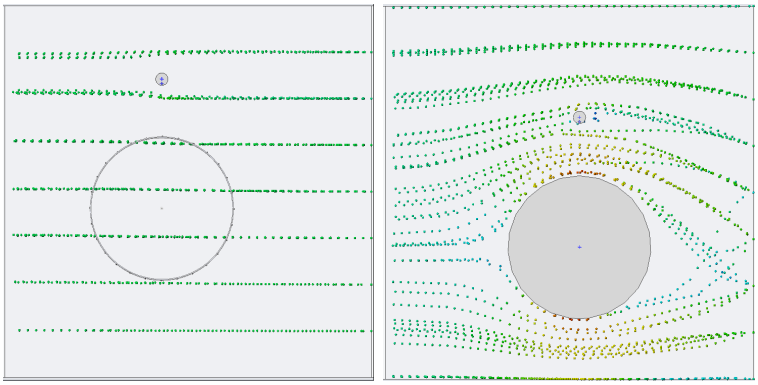

(a) (b)

Figure 23: Airflow around two different electrode configurations. (a) At the mesh cylinder, the airflow is continuous. (b) Solid cylinder, the airflow is concentrated between the electrodes.

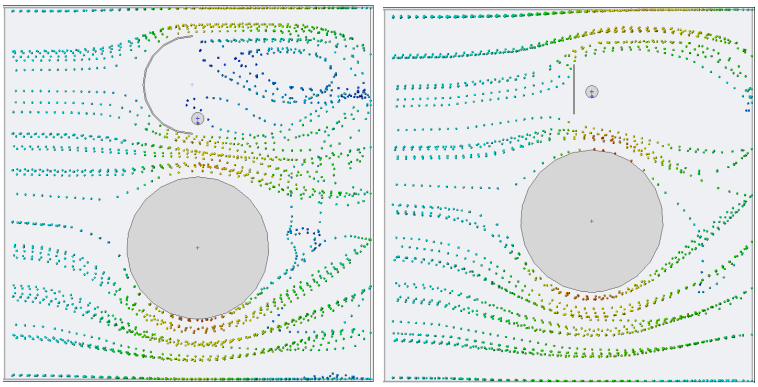

(a) Round windshield (b) Rectangular wind shield

Figure 24: A wind shield is applied to prevent the disturbance of the electrospraying process by the wind.

A drawback in previous experiments with the self adjusting multinozzle system was the disturbance of the electrospraying process by the wind. In figure 24, wind shields are placed to prevent the Taylor cones from being disrupted. With this configuration, the creation of Taylor cones will be stable while the transport of the charged droplets is enhanced because of the locally increased wind speed. A round shape results in the highest wind speed, therefore, this shield will be used for wind experiments, as can be observed in figure 24a.

4.3. Power density

Once the electrode configuration has been defined, a certain area will be available where the wind will be able to act on the charged droplets. Recalling Betz' law from section 1.2.2, the maximum power which can be converted by the wind at a certain area is given by

$$P_{max} = \frac{8}{27} \cdot A \cdot \rho_{air} \cdot v^3$$

where A is the area, ρ_{air} the density of air and v the wind speed. The area is restricted by the dimensions of the test setup, which is the space between the ground-electrode and the liquid channel. This area will be decreased by the wind shield, which prevents the cones being disturbed by the wind. In figure 25, a sketch is presented to show the dimensions of the available area. The area is calculated by multiplying the liquid channel length by the distance between the ground-electrode and the wind shield. The calculated power at this area will be used as a reference for further experiments.

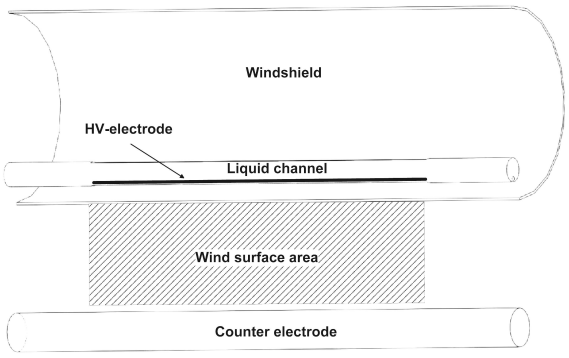

Figure 25: The available area where the wind can act on the charged droplets is given by the liquid channel length and the distance between the ground-electrode and the wind shield.

4.4. Conclusion

In this chapter the geometry of the experimental setup has been defined. The optimal size and shape of the ground-electrode has been obtained by computer simulation and experiments. On one hand, a cylindrical electrode with a large ratio, regarding to the HV-electrode, creates a strong field concentration at the location of the spraying liquid, which is favorable for the electrospraying process. On the other hand, this large ratio increases the terminal electrostatic velocity significantly.

From the airflow simulation can be concluded that the large cylindrical electrode increases the wind speed locally at the location where charged droplets are formed. From charging experiments, which will be explained in detail in chapter 6, can be concluded that the terminal electrostatic velocity is the dominant factor in terms of the electrode size. The advantage of a large cylindrical electrode according to increased wind speed is outweighed by the large v_T. For further experimentation, the solid cylinder with a ratio of 8 will be used as the ground-electrode at a distance of 42 mm. On one hand, this distance will provide a sufficiently large surface area for

the wind to transport the charged droplets. On the other hand, the applied potential is expected to be below the inception of corona discharge in the surrounding air.

Applying a windshield prevents that the charging process is disturbed and contributes to the local increase of wind speed. The electrode configuration and wind shield determine which area will be available for the wind to act on charged droplets. This area will be used as a reference for the maximum power which could be extracted according to Betz' law.

5. Electrospraying experiments

In this chapter, the charging setup, which was obtained in chapter 4, will be examined with respect to the electrospraying properties. As briefly mentioned in section 3.6, the setup will be self adjusting. The produced current and number of Taylor cones varies, as the flow rate and applied potential are adjusted. In paragraph 5.1, system requirements will be given, derived from the previous chapters. Section 5.2, experiments will be described to verify which factors are necessary to meet these requirements. This will result in a set of parameters which will be used to investigate the output power of the EWICON system, described in chapter 6. In paragraph 5.3, several factors will be described which affect the accuracy of the measurements. In section 5.4, conclusions are obtained for further experimentation with the complete EWICON setup.

5.1. Requirements

From the theory discussed in chapter 3 and the electrical properties described in chapter 4, the following requirements are given for a high power output of the EWICON system. The relations between input and output are investigated with the experiments from this chapter and the output power will be verified in the next chapter.

- The number of cones should be large, in this way the maximum available area is utilized which increases the power density
- The flow rate should be low to produce small droplets which increases the CMR
- The electric field should be restricted to prevent that charged droplets will be attracted back to the electrode

5.2. Experiments

To satisfy the conditions described above, a balance between flow rate and potential has to be acquired. The power density has to be as large as possible while maintaining a low potential and a low flow rate. In the experiments was attempted to create multiple cones, preferably in the cone jet mode. Firstly, in section 5.2.1, the relation between liquid flow rate and the number of cones is investigated. Subsequently, in section 5.2.2, the hysteresis effect will be described and how the electrospraying process benefits from this effect. From the onset potential, can be verified if equation 28 can be applied to a multinozzle system. This will be explained in section 5.2.3. Finally, in section 5.2.4, the effect of polarity and applied potential on electrospraying will be investigated. From the equations in section 3.4 can be verified if the electrospraying process occurs in the cone jet mode.

In the experiments, will be referred to stable spraying. This is defined by a continuous and visual stable Taylor cone which produces a non fluctuating current and monodisperse droplets.

5.2.1. Number of cones and flow rate

To utilize as much as possible of the available wind surface area, a large number of cones has to be established. When the potential is at a fixed value, the number of

cones is dependent on the flow rate as depicted in figure 26. The expected value of the number of cones (n) was obtained by fitting the data points in Matlab, resulting in

$$n \approx 1.6 \cdot ln(Q_l) - 1.2 \tag{30}$$

in which Q_l is the liquid flow rate in ml/hr. It is important to note that, when the average number of cones from various experiments was calculated, the standard deviation is larger than 0.5 at any given flow rate which means that there could be a variation of one cone from the expected number. From figure 26, it can be concluded that the variation in number is large at low flow rates and decreases with increasing flow rate. The number of cones is also dependent on the voltage as will be described in the next experiments.

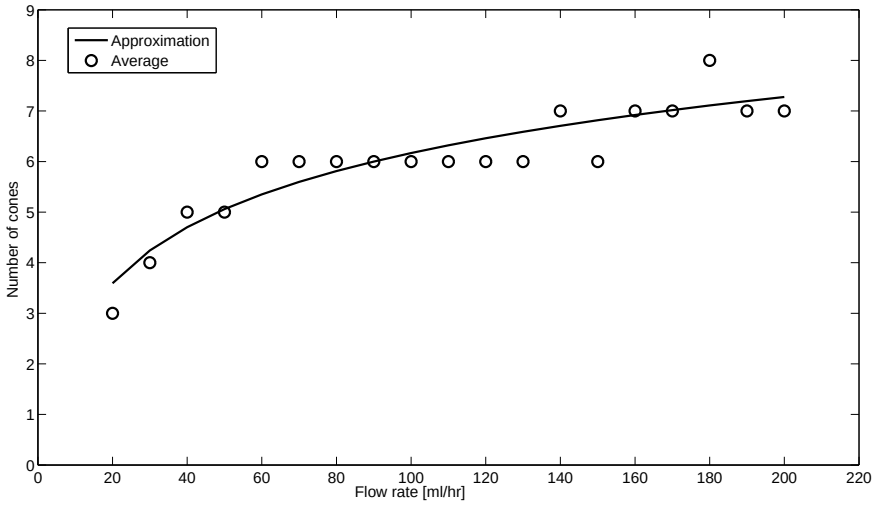

Figure 26: Expected number of cones as a function of flow rate at a potential of 23 kV. This number can be estimated by formula 30.

5.2.2. Hysteresis effect

During the experiments, the following effect was observed. If a certain threshold potential was required to initiate electrospraying, and the potential was reduced, a lower than the original onset potential was still sufficient to maintain electrospraying. This is known as the hysteresis effect, which has also been described in literature [10]. Figure 27 illustrates this effect.

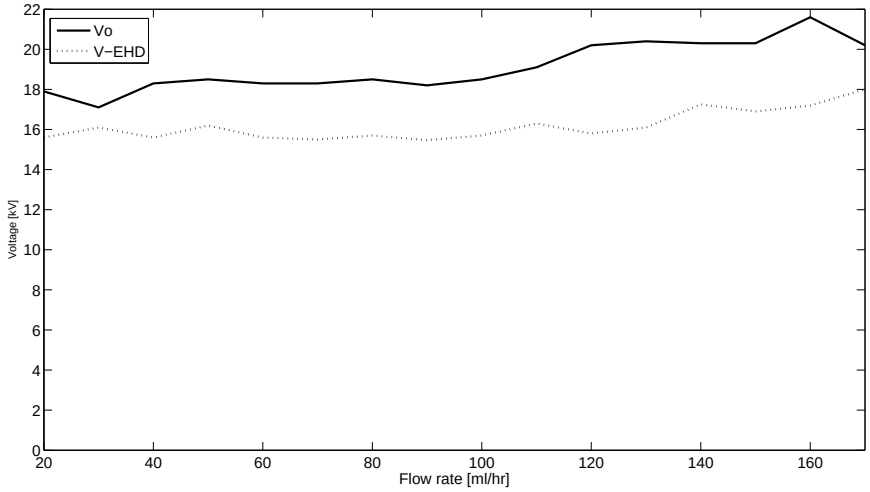

Figure 27: Hysteresis effect. At a certain potential Vo the first stable cone is formed. This cone disappears when the potential is decreased below $V - EDH$.

This effect could be useful because the number of cones increases with increasing potential. At a certain potential there will be a certain number of cones. To increase the number of cones, the potential is first raised and subsequently decreased to the initial value. Due to the hysteresis effect, the number of cones will be higher than the initial number. Experiments confirm this hypothesis as is illustrated in table 3 and figure 28. The number of cones is recorded while the initial potential V_i, was increased by 20 % and subsequently decreased to its original value.

From these experiments can be concluded that the number of cones will increase with applied potential. However, when the potential is raised, the spraying process becomes increasingly unstable. To create a large number of Taylor cones while maintaining a low potential, the hysteresis effect could be applied. At this low potential, the droplets are smaller and the electric field is lower which is advantageous in terms of v_T and CMR.

Table 3: Number of cones at initial potential, 20% increased potential and decreased to initial potential again.

potential	Number of cones
V_i	5
$1.2 \cdot V_i$	8
V_i	7

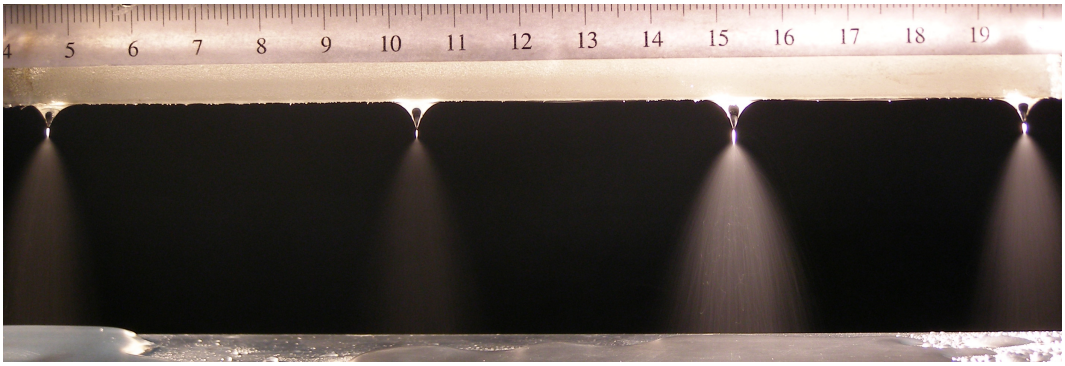

(a) 4 cones occur at an initial potential of 19 kV.

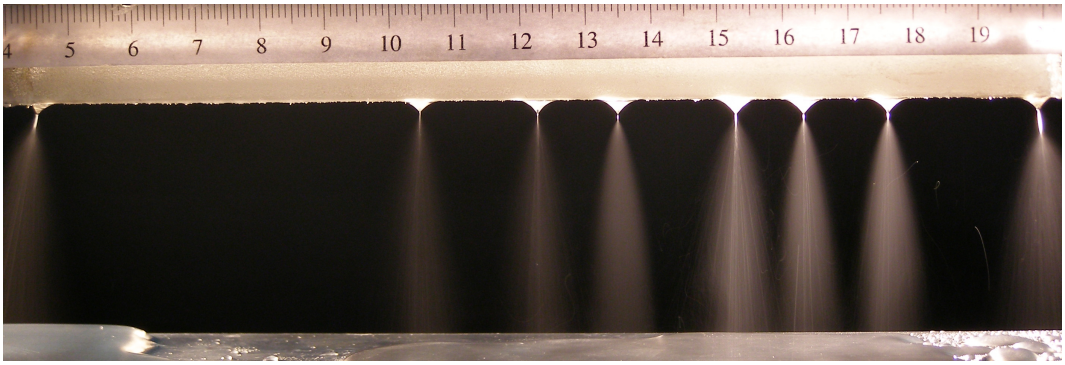

(b) 8 cones form when the potential is increased to 25 kV.

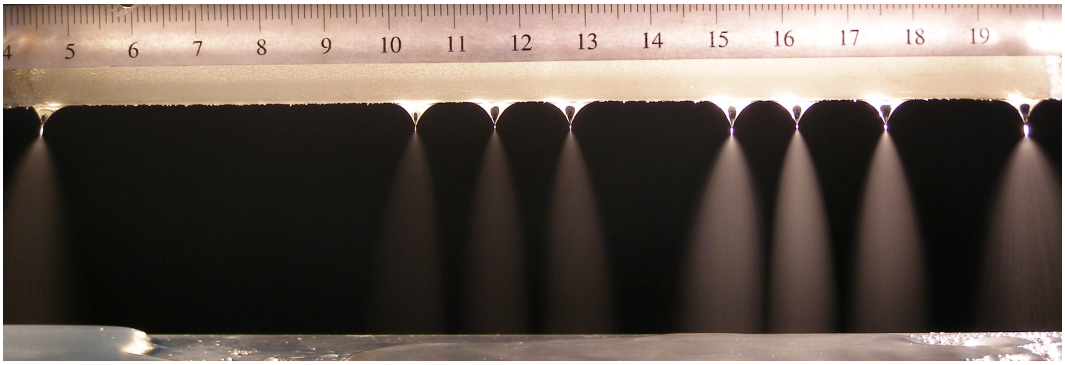

(c) 19 kV with 8 cones

Figure 28: A higher number of Taylor cones can be achieved at the same potential, utilizing the hysteresis effect i.e. shortly increase the potential.

5.2.3. Onset potential

This experiment has been conducted to verify if equation 28 from paragraph 3.5 could be applied at the multinozzle setup. This formula is based on a single nozzle setup with a conductive needle perpendicular to a plate.

$$V_0 = A \cdot \sqrt{\frac{2 \cdot \gamma \cdot r \cdot cos(\theta)}{\epsilon_0}} \cdot ln\left(\frac{4 \cdot h}{r}\right)$$

In the multinozzle system, r is represented by half the liquid channel width, the half angle was obtained from experiments, as well the onset potential. From the average of all measurements, a value of 1.17 is obtained for A. The calculated value of V_0 is compared to the average measured V_0. Results are given in table 4. When the onset potential is used as an input parameter in Lorentz, the field plot shows a good agreement with E_0 at a distance r from the electrode, see figure. This is also the case when the single needle setup is simulated, see appendix C.

Table 4: Calculated and experimental value of V_0. Formula 28 can be used to estimate the potential where the first stable cone occurs. Before all cones are stable, a higher potential is required and this equation no longer holds.

Parameter	Value
$V_0 - experiment$	19.2 kV
$\theta - experiment$	20.26 deg
$E_0 - calculated$	$1.67 \cdot 10^6$V/m
$V_0 - calculated$	18.7 kV

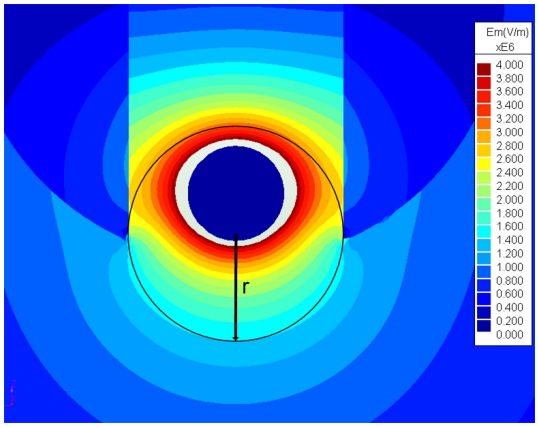

Figure 29: Field plot in Lorentz. at a distance r from the electrode, the value of E_0 can be observed, which agrees reasonably with the calculated value. A comparison of field plot results and calculation results is given in appendix C.

It is important to note that the experimental value of the onset potential was recorded, when only one stable cone was observed. A higher potential is required for all cones to be stable. In figure 27 can be seen that the onset voltage also increases with flow rate.

5.2.4. Polarity

Different types of aerosol were observed when the polarity was changed from positive to negative, as depicted in figure 31. A positive applied potential resulted in a wide aerosol and the current per cone will vary with magnitude. When a negative potential was applied, a narrow aerosol was observed and the current per cone was independent of the applied potential. These observations are summarized in figure 30, where experimental values of positive as negative potential are given each at 25 and 28 kV. The calculated theoretical current from equation 21 is also presented in this figure.

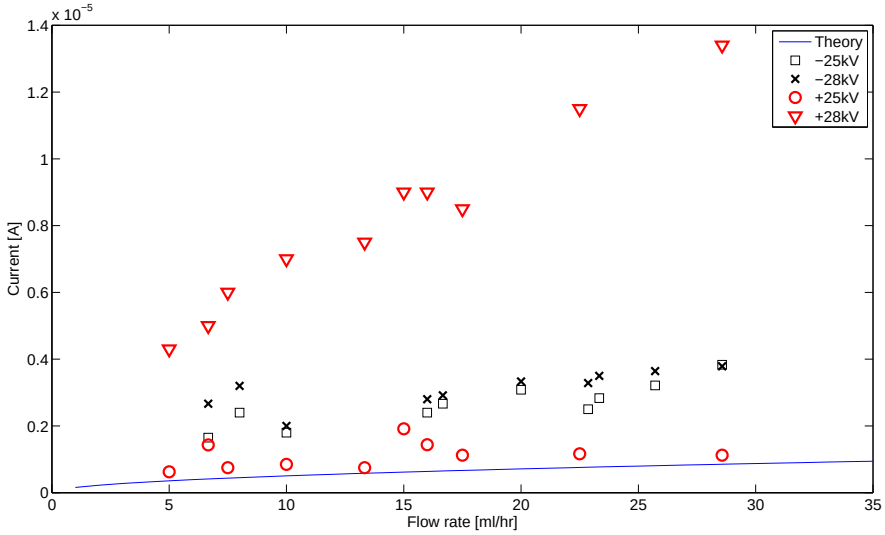

Figure 30: Current per cone at different polarity and value of the applied potential, as a function of flow rate. At +25 kV the relation between current and flow rate is similar to the theoretical relation, assuming the spraying process occurs in the cone jet mode.

This experiment shows that at 25 kV, the current of the negative potential is higher than the current at a positive potential. While the current per cone and the number of cones increases, as the positive potential rises, it remained constant at the same increase of the negative potential. The utilized surface area is much larger at positive voltage, due to the wide aerosol and the increasing number of cones. Experiments with the complete EWICON setup will have to demonstrate which polarity will be most suitable in terms of displacement of droplets.

The positive 25 kV current suggests that the cone jet mode is achieved, however, this can not be confirmed unless the droplet size is known. It was observed that the current was stable and small uniform droplets were obtained. This in contrast with 28 kV, where the current fluctuated and no stability was observed in cone formation and droplets size. The observed noise indicates possible corona discharge.

When closer observations were made, regarding to the negative potential, corona discharges were visible at the base of every cone. The measured current is partly caused by discharge and will not contribute to the charging process. In general, the inception voltage of negative corona is lower than positive corona [23] which explains the above mentioned observations.

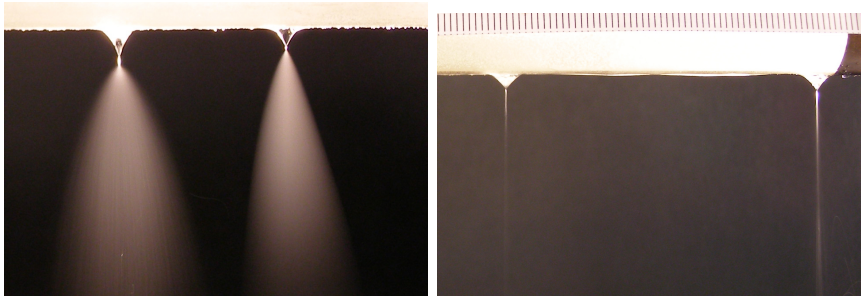

(a) + 25kV (b) - 25 kV

Figure 31: Aerosol at different polarity of the applied potential. A cone formed by a positive applied potential, produces a wide aerosol of charged droplets.

5.3. Factors affecting stable electrospraying

During the experiments, it was observed that certain factors affected the measurements. This resulted in unstable electrospraying, fluctuating currents or leakage currents. Three main factors are described below.

5.3.1. Humidity

The humidity of the surrounding air has a strong influence at the measurements. At a relative humidity of 70 percent (at 20 degrees Celsius) or higher, an increasing leakage current is observed. At 80 percent, the electrospraying process is disturbed and flash over occur between the electrodes. As a consequence, there is a strong fluctuation of the spraying current, which makes accurate measurements impossible. Apparently, the water vapor which is present in the surrounding air interacts with the electric field and the electrospraying process. This suggests that an EWICON system could not operate when the absolute humidity of the air is more than 12 g/m^3, which occurs on average 35 days per year in the Netherlands. For more information about the humidity of air, see appendix D.

5.3.2. Liquid flow

The liquid flows from the syringe pump through the flow distributor into the porous material, where it creates an uniform liquid film along the electrode. A small disturbance in flow rate caused by the inhomogeneous material can change the flow rate in an individual cone. This will affect the produced spraying current or the spraying mode.

5.3.3. Electric field

The electric field has to be uniformly divided along the liquid channel. In this way, the mode of electrospraying is similar for every cone. At the current setup the electrode edges cause a local increase of the electric field. At these points the spraying mode is different which causes an unstable situation. The electrode should be in contact with the spraying liquid and has to be embedded into the porous material.

5.4. Conclusions

From the results of the experiments, empirical relations have been obtained between the input parameters (potential and flow rate) and the output (current per droplet and number of cones). The following conclusions can be derived from the experiments .

- The number of cones can be increased by increasing the flow rate of the liquid and by increasing the applied potential.
- The hysteresis effect can be used to increase the number of cones while maintaining the same potential and flow rate by shortly increase the potential and subsequently decrease to its original value.
- The onset potential can be estimated by the theoretical equations which are used for a single needle configuration. However, this relation will not hold, when more cones appear.
- The polarity affects the shape of the aerosol and negative polarity results in corona discharge.
- At a potential of plus 25 kV, it may be possible to achieve cone jet mode. At higher potential, a different less stable, mode occurs.

To obtain the maximum power density as described in paragraph 4.3, the flow rate should be high to generate a large number of cones. From the above mentioned discussion, this number could be increased using the hysteresis effect. The applied potential has to be as low as possible, in order to generate stable spraying as well minimizing the terminal electrostatic velocity. For further experimentation, the flow rate will be set between 100 and 160 ml/hr. The applied potential will be set between 23 and 25 kV(depending on flow rate), after a short increase to 28kV. Both positive as well as negative polarity will be further examined in the final complete system.

6. Complete EWICON system

In the previous chapters, the theory of the self adjusting multinozzle system has been explained. From experiments and simulations, electrospraying configurations were tested and optimized and electrospraying parameters were analyzed.

In this chapter, the charging system will be applied in a complete EWICON system. In paragraph 6.1, hypotheses about the output power, derived from the experiments in chapter 5, will be proposed. The experimental setup will be presented in paragraph 6.2, which is of type B as has been explained in chapter 2. In section 6.3, results of the conducted experiments will be presented, where the output power is calculated at different input settings. Finally in section 6.4, the system efficiency will be compared to a similar system, followed by conclusions about the performance of the self adjusting multinozzle system in section 6.5.

6.1. Hypotheses

From the previous chapters, relations have been investigated between the applied potential, flow rate and the expected number of cones. From these relations, the following hypotheses are proposed according to the output power.

- Increased flow rate leads to an increased power
- Less power will be produced with a negative charging potential, compared to a positive potential
- Increased potential leads to increased power
- The most important parameter is the number of cones to obtain maximum power
- Power increases with wind speed

6.2. Setup

The EWICON system type which will be applied is a type B, as explained in section 2.3. The complete charging system is insulated and the earth acts as a charge collector. As a consequence, all electrical equipment has to be powered by a battery. The setup consists of a battery, inverter, HVDC source, pump and the charging system, as described in chapter 4. All components are placed on a metal plate which is supported by ceramic insulators.

The insulated metal plate acts as a capacitor which is charged by the removal of the charged droplets. The polarity of the droplets is opposite from the charging electrode. Consequently, when for example negative droplets are being removed by the wind, a positive potential rise occurs at the metal plate. The potential rise on the system has no influence the spraying process because the charging potential rises correspondingly. In other words, the potential difference between the charging system and the plate remains constant. An electrostatic voltmeter is connected to the plate to measure this potential rise. The components of the EWICON system are schematically depicted in figure 32. Detailed photographs of the actual test setup are depicted in appendix E.

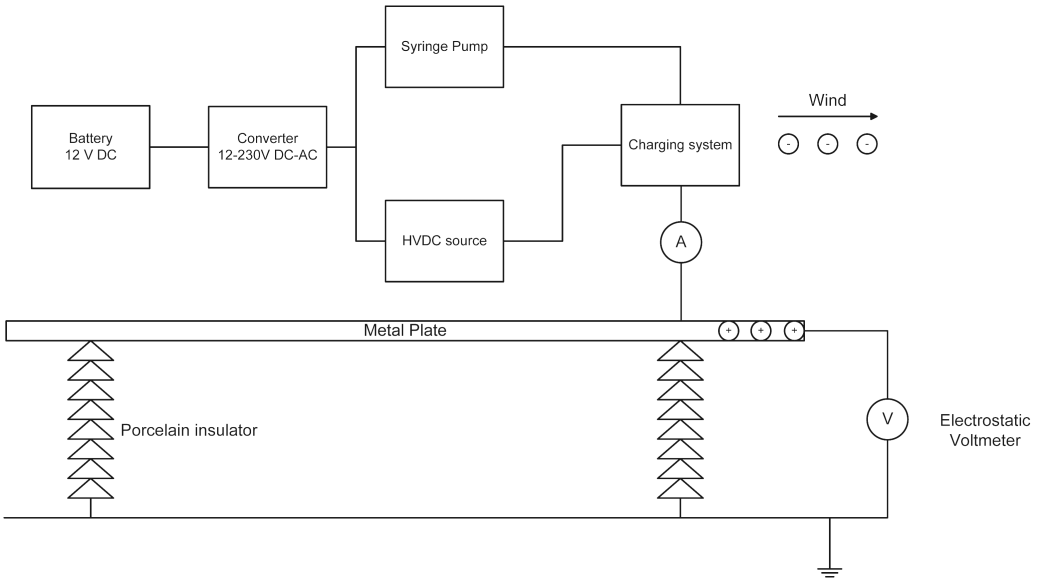

Figure 32: Schematic representation of the EWICON system. All components are on the metal plate insulated from earth. The wind displaces negative charged droplets, which causes a positive potential rise of the plate.

6.2.1. Test procedure

The experiment was performed in the steps described below. For safety reasons it is important that the steps are followed in the right order and the plate is always connected to earth while the parameters are adjusted.

- Ensure that the plate is connected to earth
- The wind generator is set at the desired wind speed
- The flow rate of the pump is established
- The potential is set to initiate electrospraying
- The plate is disconnected from earth
- The potential rise can be observed with an electrostatic voltmeter

When both time and potential are recorded, the charging current (i_{charge}) can be obtained from equation 31.

$$i_{charge} = C_{EWICON} \cdot \frac{dV}{dt} \tag{31}$$

where C_{EWICON} is the capacitance between the metal plate and earth (130 pF) and dV is the potential rise of the metal plate. The output power can be calculated at every moment, by multiplying the potential with the corresponding charging current.

The system can be modeled by an equivalent circuit of a current source with an internal resistance $R_{internal}$, which has a value of the potential divided by the current at maximum power. This value is also equal to the load resistance R_{load} to obtain maximum power transfer. The insulator losses are represented by R_{loss} (20TΩ) and the capacitance of the EWICON system is given by C_{EWICON}. The circuit is depicted in figure 33.

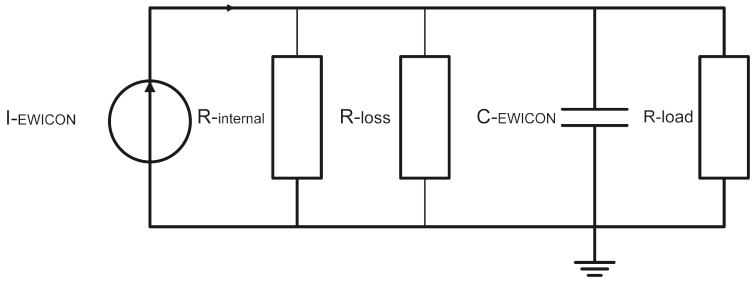

Figure 33: Equivalent circuit of the EWICON system. The EWICON system can be modeled by a current source with an internal resistance which is equal to the load resistance to obtain maximum power transfer. The capacitance is represented by the insulated metal plate and the losses are caused by the insulators.

6.3. Experiments

To test the hypotheses from paragraph 6.1, three experiments have been conducted to determine the output power. Both potential rise and time were recorded. With equation 31, the current can be determined and the power can be calculated by multiplying this current with the corresponding potential. The load resistance can be obtained by dividing the potential by the output current. An example is given in figure 34 together with table 5

Table 5: Calculated values for power and load resistance. From the maximum power, the load resistance can be calculated to obtain maximum power transfer.

potential $[kV]$	Current $[\mu A]$	Power $[mW]$	R-load $[G\Omega]$
4	0.4	1.6	10

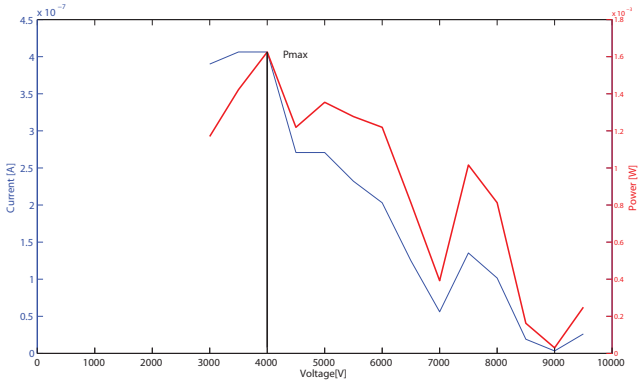

Figure 34: Output current and power at a charging potential of 25 kV, a flow rate of 100 ml/hr and a wind speed of 12 m/s. the maximum power can be observed at 4 kV.

6.3.1. Flow rate

In the first experiment the flow rate was changed from 100 to 200 ml/hr. The charging potential was set at 25 kV and 5 Taylor cones occurred. The wind speed was 12 m/s and the output power is calculated and presented in figure 35, as a function of potential. From this figure it can be concluded that, when the flow rate is doubled, the maximum output power increases 1.7 times. This means that twice the mechanical power has to be supplied to obtain less than two times the output power. This result could be expected, since the spraying current is proportional with the square root of the flow rate.

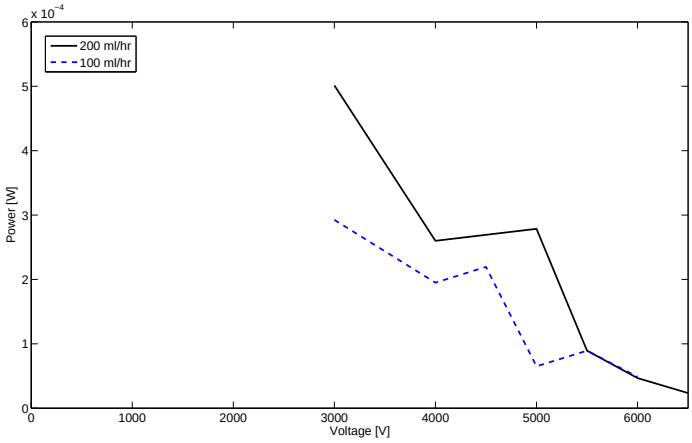

Figure 35: Output power with different flow rates. The increase in flow rate leads to an increase in output power. However more power will be required as is gained.

6.3.2. Charging potential

In figure 36, the potential level is varied as well as the polarity. The liquid supply is 100 ml/hr and the wind speed was set at 12 m/s. As expected the output power was very low with negative polarity. At the positive polarity, the increase in potential leads to an increase in output power of 1.7 times.

6.3.3. Number of cones

The number of cones was increased by 2 at this experiment. The charging potential and wind speed are 25kV and 12 m/s respectively. Figure 37 shows a large increase in power as the number was increased from 5 to 7 cones.

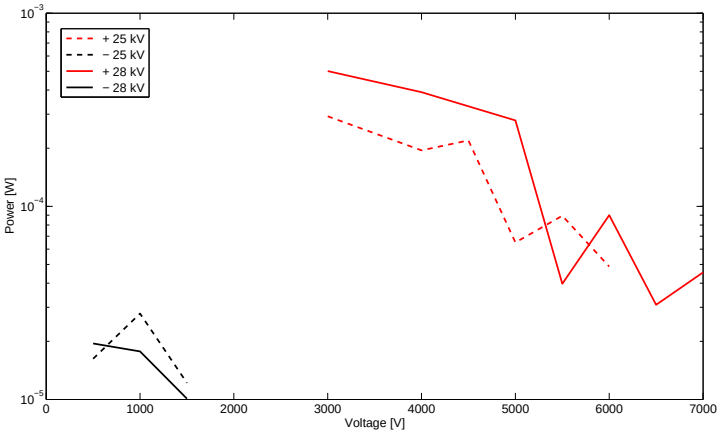

Figure 36: Output power at positive and negative charging potential. A negative polarity results in a low output power. An increase in positive polarity results in an increase in output power.

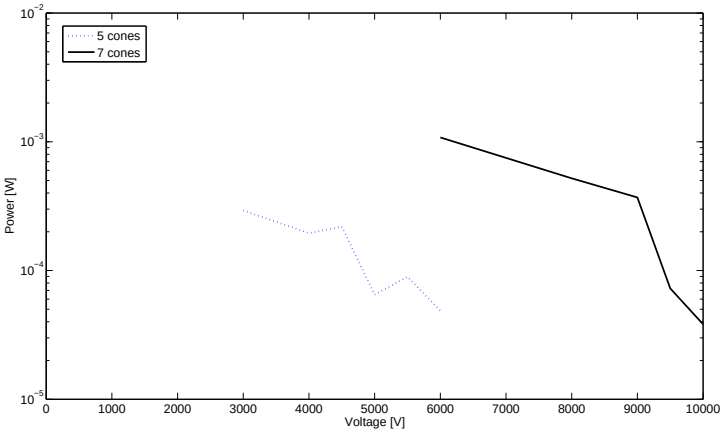

Figure 37: Output power at 5 and 7 Taylor cones. At a higher number of cones, significantly more power is generated.

6.3.4. Wind speed

In the last experiment, the wind speed was varied at a flow rate of 100 ml/hr and a charging potential of 25 kV. Only the maximum output power is given in figure 38 as a function of the wind speed. The experimental data is fitted in Matlab with a cubic polynomial function given by

$$P_{out} = 2.8 \cdot 10^{-4} \cdot v^3$$

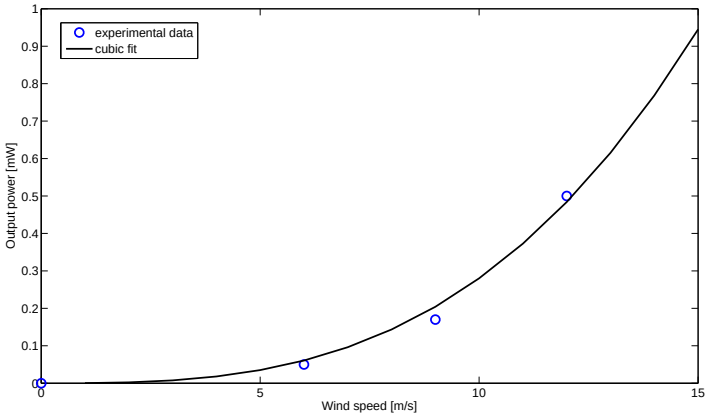

Figure 38: Output power at a wind speed of 6, 9 and 12 m/s respectively. The power increases with wind speed and can be fitted with a cubic polynomial function.

Table 6 summarizes the maximum output power from figure 35 to 38. From this table, we can say that the hypotheses in paragraph 6.1 are confirmed. The output power increases most, when more cones are present. Furthermore, increasing the flow rate, potential and wind speed will lead to an increased output power. In the 9^{th} row of this table, a more accurate measurement was performed, in which the time and potential were recorded with a camera. This measurement was also used for the example in figure 34. It will be assumed that, if the other experiments will be recorded more accurately, the same relations will be observed, however the potential where maximum power occurs will be different at the more accurate measurements.

Table 6: Comparison of maximum output power with various input parameters.

Charging potential [kV]	Flow rate [ml/hr]	Wind speed [m/s]	Number of cones	Output power [mW]
25	200	12	5	0.5
25	100	6	5	0.05
25	100	9	5	0.17
25	100	12	5	0.29
28	100	12	5	0.5
-25	100	12	5	0.03
-28	100	12	5	0.02
25	100	12	7	1.01
25	100	12	5	1.61

6.4. System efficiency

To asses the performance of the self adjusting multinozzle system, it will be compared to a 6-needle configuration which has been investigated by Dr. ir. Djairam [5]. This configuration had been tested with the same spraying liquid and wind speed. Firstly, the efficiency of the multinozzle system has to be determined, given by

$$\eta = \frac{P_{out}}{\sum P_{in}} \tag{32}$$

where P_{out} is the calculated maximum output power. P_{in} is the sum of the maximum recoverable power (Betz), the electrical power end the mechanical power, given by

$$\sum P_{in} = P_{max} + P_{electrical} + P_{mechnical} \tag{33}$$

$P_{mechanical}$ is the energy required for pumping the liquid to a certain height (h) for a given flow rate, and given by

$$P_{out} = Q \cdot \rho \cdot g \cdot h$$

where Q is the flow rate in l/hr. The electrical losses are calculated by multiplying the charging potential with the current which flows back from the charging system to the metal plate. This current is caused by charged droplets which are not removed from the system by the wind. To compare the self adjusting multinozzle system with other configurations described in [5], the EWICON Performance Index (EPI) will be introduced. With this number particular charging system can be rated, according to output power, efficiency, surface area and flow rate. The EPI is given by

$$EPI = \log\left(P_{out} \cdot \frac{\eta}{A \cdot Q_l}\right)$$

where Q_l is the flow rate in l/hr.

In table 7 the 6-needles configuration is compared with the 5-cones experiment at 25 kV and 100 ml/hr. The mechanical power is calculated assuming that the liquid is pumped to a height of 2 meters. At the multinozzle system the current flowing back from the charging system to the plate is estimated at 2 μA.

In the third row of table 6, values are given for an ideal self adjusting multinozzle system under the following assumptions:

12 cones will produce 24 mW at a flow rate of 100 ml/hr and no electrical losses occur (all droplets will be removed by the wind).

Table 7: Comparison between a 6 needle system and the self adjusting multinozzle system and an ideal multinozzle system.

	P_{out} $[mW]$	P_{max} $[mW]$	$P_{electrical}$ $[mW]$	$P_{mechanical}$ $[mW]$	P_{in} $[mW]$	Q $[l/hr]$	A $[cm^2]$	η [%	EPI
6 needles	12.5	1479	0.1	0.622	1480	0.12	24	0.84	2.20
5 cones	1.6	2959	50	0.519	3009	0.1	48	0.05	0.74
12 cones	24	2959	0	0.519	2959	0.1	48	0.81	2.61

6.5. Conclusions

From the charging experiments of the EWICON system, it can be concluded that the highest output power is generated at the highest number of Taylor cones. Increasing the flow rate also results in a rise of the output power, however, less electrical power is generated than extra mechanical power needed for the spraying liquid supply. At a negative charging potential, it is possible to generate an output power, however this power is a factor 10 smaller than at a positive potential. As expected, the power increases with wind speed. This relation could be approximated with a cubic polynomial function.

The system efficiency is low compared to a 6-needle configuration as well as the EPI. The electrical losses are significantly higher than the maximum output power. Only in an ideal situation, if all droplets could be removed by the wind and 12 cones will produce 24 mW, the efficiency and EPI are comparable to the needle system. If this ideal system would be scaled to obtain 100 watts of electrical energy, an area of 100 square meters would be required.

7. Conclusions and recommendations

In this chapter, conclusions are presented on the feasibility of an EWICON system with the self adjusting multinozzle electrospraying technique. Firstly the conclusions of each chapter are presented in section 7.1 followed by a general conclusion about this research. Secondly, in section 7.3, recommendations for future work will be given.

7.1. Conclusions per chapter

The EWICON has been discussed. It is a system that converts wind energy directly to electrical energy. No moving or rotating parts are required which has advantages compared to conventional wind turbines, with respect to maintenance costs, noise and scaling. The working principle of the EWICON is the potential energy rise, resulting from the work that is done by the wind on a charged droplet in an electric field. The charged droplet creation is done by a self adjusting multinozzle electrospraying technique.

To create small highly charged droplets in a self adjusting multinozzle system, electrohydrodynamic atomization has been applied. From the theory on EHDA, the relation between liquid properties, droplet size, charge and current can be calculated. It can be concluded that the desired droplet size should be as small as possible and that the charge per droplet should be high. Having implemented this, a large amount of charge could be displaced per unit of time and the number of charged droplets that are attracted back to the electrodes, is small. To create highly charged, monodisperse and small droplets, from which the current and size can be calculated, the cone jet mode is preferable. From experiments can be concluded that the optimal spraying liquid for application in this particular self adjusting system, consists of 30% ethanol and 70 % demineralized water. Theoretically, a high charge to mass ratio can be obtained and in practice, stable electrospraying was achieved.

Using simulation and experiments, concerning the electric field and airflow, an electrode configuration was constructed. The HV-electrode is embedded in a porous material, which is in contact with the spraying liquid. The diameter ratio between this electrode and the counter electrode is determined by the terminal electrostatic velocity and the electric field concentration at the spraying liquid. The optimal ratio appeared to be 8. The electric field is concentrated such, that stable electrospraying occurs and the terminal electrostatic velocity is minimized. Thus, reducing the number of charged droplets which will be attracted to the system.

From the electrospraying experiments, it can be concluded that the number of cones is one of the most important aspects determining the maximum power density at a given surface area. An increase in flow rate as well as charging potential, leads to an increase in the number of cones. A drawback of the increased flow rate is that it will also increase the required mechanical input power. An increased potential results in corona discharges, negatively affecting the spraying mode. In an optimal situation, a large number of cones are created while maintaining a low flow rate and a low potential. This can partly be achieved by making use of the hysteresis effect i.e. a momentary increase of the potential. Furthermore, it was observer that a positive potential generates more cones and a larger aerosol per cone compared to a negative potential.

The results discussed above, have been applied in a complete EWICON system of type B. The electrical potential increased as charged droplets were removed by the wind. This is a significant improvement compared to previous research on a self adjusting multinozzle system. However, due to the inability of removing all charged droplets by the wind, the output power was lower than the required electrical input power. To judge the performance of the self adjusting multinozzle system, it has been compared to a multi needle configuration. The current multinozzle setup has a low efficiency compared to the needle system. However, when improvements are made regarding the charged droplet displacement and an ideal formation of 12 cones occurs, the self adjusting multinozzle system would have the same specifications as the needle system. this offers perspective for further research.

7.2. General conclusions

In a self adjusting multinozzle system a very delicate balance exists between a large number of parameters. The number of cones and the spraying mode are sensitive to small system changes. Thus, the output current, stability, droplet size and charge are affected. Those changes are caused by the system construction and external influences. In this stage of research, the self adjusting properties are not directly an advantage of this technique, because the system could not be forced into a particular mode.

Due to inhomogeneity of the porous material the flow rate is not equally distributed. Combined with the increased field strength of the HV-electrode edges, the flow rate and electric field, and thus the mode and produced current per cone differ.

The humidity of the surrounding air affects the electrospraying process. Above 12 g/m^3 leakage currents occur that are in the same order of the spraying current. At an absolute humidity of more than 14 g/m^3, the leakage currents increase even more and flash overs could occur.

Despite the low conversion efficiency compared to a multi needle system, the performance of the self adjusting multinozzle system has been largely improved. When the system would be able to remove all charged droplets and the power density is improved, the self adjusting multinozzle technique becomes an interesting option for implementation in an EWICON system.

7.3. Recommendations

The EWICON system in general and the self adjusting multinozzle technique in particular, are still in an early stage of development. The ultimate goal is to construct an EWICON system which can compete with conventional wind turbines, making use of natural resources.

In general, more experiments have to be conducted, to clarify all parameters affecting the self adjusting multinozzle technique.

To optimize the current setup, firstly all charged droplets have to be displaced by the wind. This could be achieved by adding an extra electrode to optimize the electric field distribution. This will result in a decrease of the terminal electrostatic velocity. Also the aerodynamic features of the setup should be improved. The wind has to be concentrated at the location of the charged droplets without affecting the formation of Taylor cones.

Another parameter which should be investigated is the liquid channel and the interaction between the spraying liquid, HV-electrode and liquid channel dimensions.

The humidity of the surrounding air will always be an influential parameter and when placing one or multiple EWICON systems in open air, it has to be taken into account. Research should be focused on the effects on the electrospraying process, as well on improving the electrical insulation.

As described in this research, the spraying liquid consists of demineralized water and ethanol. Ultimately, saline or fresh water from natural resources will have to be used. Developments in stable electrospraying techniques will determine if the EWICON system can be operated using these liquids.

If these issues are solved, a practical, large scale, implementation will have to be investigated. The liquid has to be supplied and filtered, the system has to be insulated and self supplying and the energy will have to be converted to common standards.

Appendices

A. Spraying liquid properties

In most of the EWICON experiments a mixture of 30% ethanol with 70% demineralized water is used as the spraying liquid. When water and ethanol are mixed, the density[19] and dielectric constant [17] will vary linear with the proportion of the mixture. On the other hand, the surface tension, viscosity and conductivity show a non linear relation as can be seen from figure 39. Table 8 gives an overview of all properties at different mixtures, which are used for calculation in this thesis.

Table 8: Properties of different mixtures of ethanol and water.

Volume percentage ethanol [%]	Density $[kg/m^3]$	Surface tension $\cdot 10^{-2}[kg \cdot s^{-2}]$	Viscosity$\cdot 10^{-3}$ $[N \cdot s/m^2]$	Dielectric constant	Conductivity $\cdot 10^{-4}$ $[S/m]$
0	998	7,20	0,89	78,41	2,2
1	980,61	4,75	1,4	74,16	1
20	968,08	3,80	1,8	69,25	0,8
30	951,55	3,30	2,1	64,03	0,59
40	935,21	3,02	2,3	58,52	0,5
50	917,78	2,80	2,4	52,74	0,45
60	895,32	2,62	2,3	46,75	0,4
70	868,38	2,50	2,1	40,67	0,35
80	842,48	2,38	1,8	34,7	0,3
90	815,7	2,27	1,5	29,17	0,25
100	789	2,18	1,1	24,6	0,22

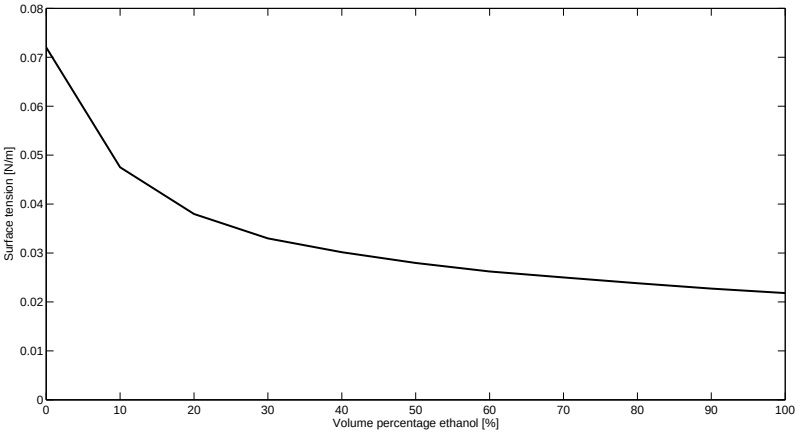

(a) Surface tension as a function of volume percentage ethanol according to [15]

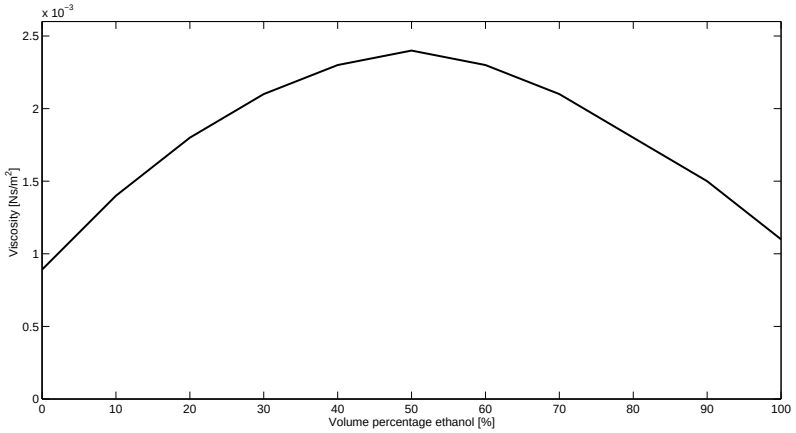

(b) Viscosity as a function of volume percentage ethanol according to [16]

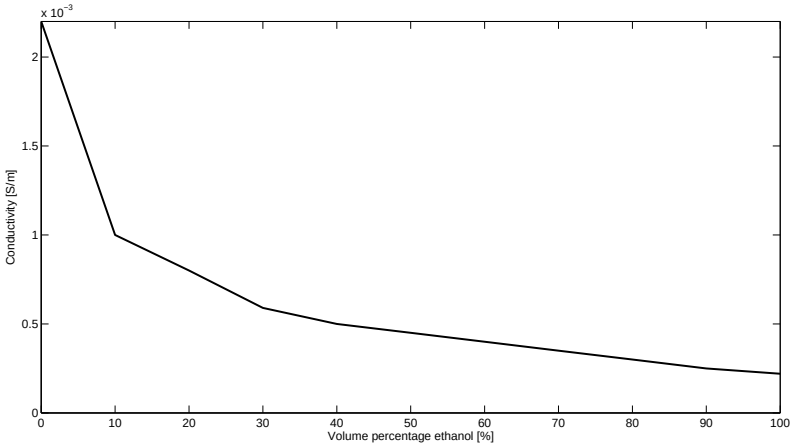

(c) Conductivity as a function of volume percentage ethanol, measured with a conductivity analyzer.

Figure 39: Relation between surface tension, viscosity and conductivity and the volume percentage of ethanol.

B. Software tools

B.1. Solidworks

Solidworks is a 3D CAD program by Dassault Systèmes SolidWorks Corp. It is a versatile design program in which it is possible to create a 3D design from a 2D sketch. It is easy and fast to create and adapt the parts and ideas for a test setup. Next to the design function a simulation tool, called FloXpress, is used to visualize the airflow around the model. The model can also be imported by Lorentz to simulate the electric field.

B.2. Lorentz

Lorentz, by Integrated Engineering Software, is a electric field simulation program based on the boundary element method(BEM). A 3D problem is divided into a mesh of 2D surfaces at the material interfaces and assigned boundary conditions. This saves computation time compared with the finite element method(FEM), where the complete volume has to be modeled to obtain the solution. Lorentz is used to calculate the electric field at the EWICON setup and illustrates the field lines in graphs and contour plots.

C. Electric field; theory and simulation

To compare the theoretical values of the electric field and the simulated field plots in Lorentz, an example is worked out from a paper of A. R. JONES and K. C. THONG [11]. In figure, 40 the calculated values of the electric field are compared to the experimental values from the experiment in question. The setup consists of a conductive needle at a high potential, perpendicular to a grounded plate. In this paper, the electric field is calculated with equation 34.

$$E_0 = \frac{\sqrt{2}V_0}{r \cdot ln\left(\frac{4 \cdot z}{r}\right)} \tag{34}$$

where V_0 is the onset voltage, r is the radius of the needle and z is the distance of the needle to the plate. To compare the test results from figure 1 with Lorentz, three configurations are reproduced. A needle with r = 0.226 mm and length of 60 mm is placed perpendicular to a plate at 1, 3 and 5 cm respectively. The applied potential is according to the experimental values in figure 40. The calculated electric field (formula 34) is given in table 9 for these three situations.

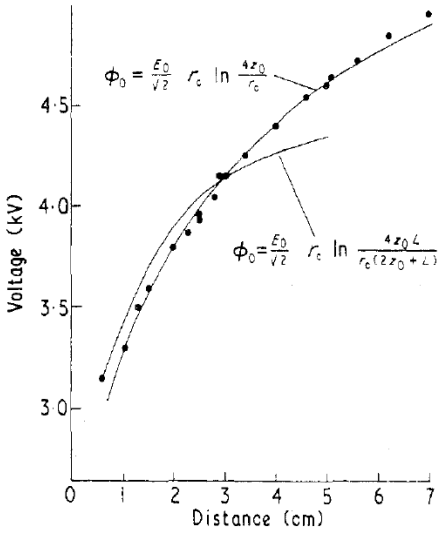

Figure 40: Voltage versus needle distance to the plate. The dots represent the experimental values and the lines the theoretical values.

Table 9: Calculated values of the electric field at different distances.

Distance [cm]	E_0 [V/m]
1	3.93E+06
3	3.87E+06
5	4.24E+06

In figure 41, the field plot in Lorentz is given for a distance of 5 cm. At the edges of the needle tip the electric filed is concentrated and the magnitude is three times the value of table 9. The value of the electric field, from the center of the needle at a distance r from the tip, agrees very well to the theoretical one. This is consistent with the two other configurations from table 9.

Formula 34 is based on an infinite plate and a infinite line of charge [11].The calculated values will show a difference according to a finite (practical) configuration. However, it results in a good approximation of the electric field strength at a perpendicular distance, equal to the radius of the needle. For a more detailed view of the electric field, especially at sharp edges, a simulation program like Lorentz is more accurate.

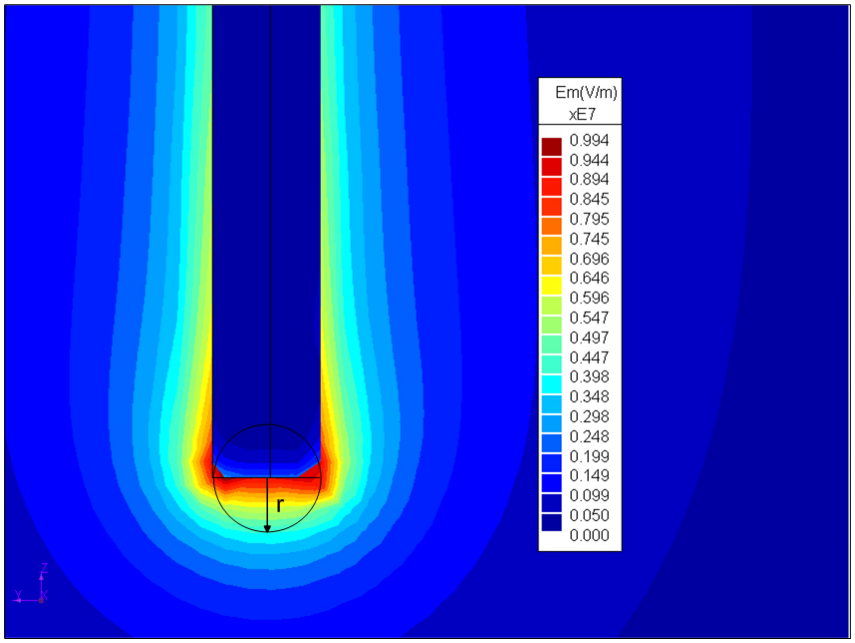

Figure 41: Field plot of a simulation with Lorentz using the same voltage and distance (5 cm) from figure 40. The value of E_0, agrees with the theoretical value at a distance r from the needle tip .

D. Humidity

As described in this thesis, the humidity of the air influences the electrospraying process and increases the leakage current. In the experiments, the relative humidity is recorded together with temperature. The relative humidity is the amount of water vapor present in a volume of air, at a specific temperature, divided by the maximum amount which can be present before condensation takes place. This maximum is presented in figure as a function of temperature[19].

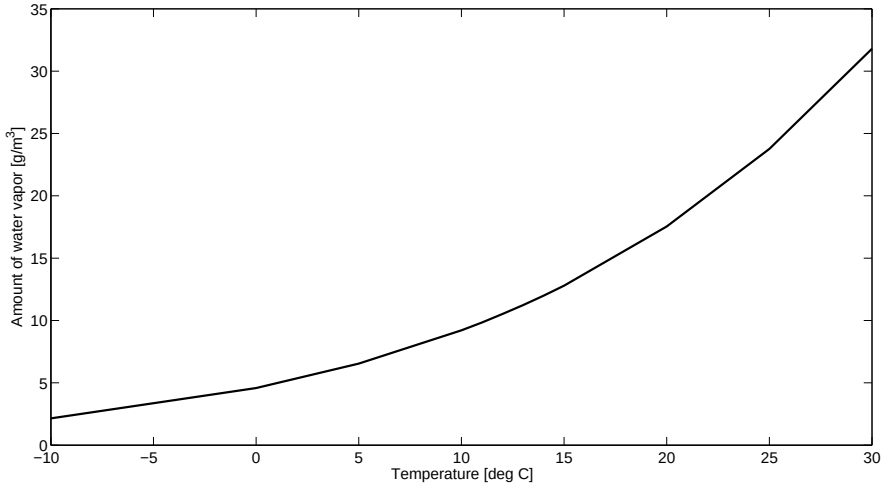

Figure 42: Maximum amount of water vapor in air at a specific temperature.

From the experiments can be concluded that at a relative humidity above 70% the EWICON will not perform well. The electrospraying process is disturbed and leakage current increase rapidly at a higher value of the relative humidity. The temperature at the experiments is almost constant, 20 ± 2 degrees Celsius. The relative humidity can be converted into the absolute humidity according to an exponential fit of figure given by

$$AH \approx \frac{RH}{100} \cdot 4.96 \cdot e^{0.062 \cdot T} \tag{35}$$

where AH is the absolute humidity, RH the relative humidity and T the temperature. In table 10 the performance of the electrospraying process is given at different values of the relative humidity at the corresponding temperature and the absolute humidity according to formula 35 .

Table 10: Influence of humidity on the electrospraying process. When more than 12 $g/m^3$of water vapor is present in the air, the electrospraying is disturbed.

Relative [%]	Absolute g/m^3	Electrospraying
<50	10	good
70-75	12-13	leakage current
>80	14.5	process disturbed, flash over

The daily average relative humidity in the Netherlands is collected at two different locations and two different years[18]. together with the temperature an estimation

can be made when the EWICON cannot operate due to high absolute humidity of the air. The threshold is set at $12 g/m^3$. Table 11 gives the results of the average days, that the EWICON possibly has to be shut down.

Table 11: Days with an absolute humidity of more than 12 g/m^3at two different locations namely, the coast and inland.

Location	Days with AH > 12 g/m^3
Inland	28
Coast	36

E. Experimental setup

In this appendix, photographs of the experimental setup for this research are presented. Firstly, the complete setup is presented followed by a more detailed picture of the charging system as well photographs of the syringe pump and electrostatic voltmeter.

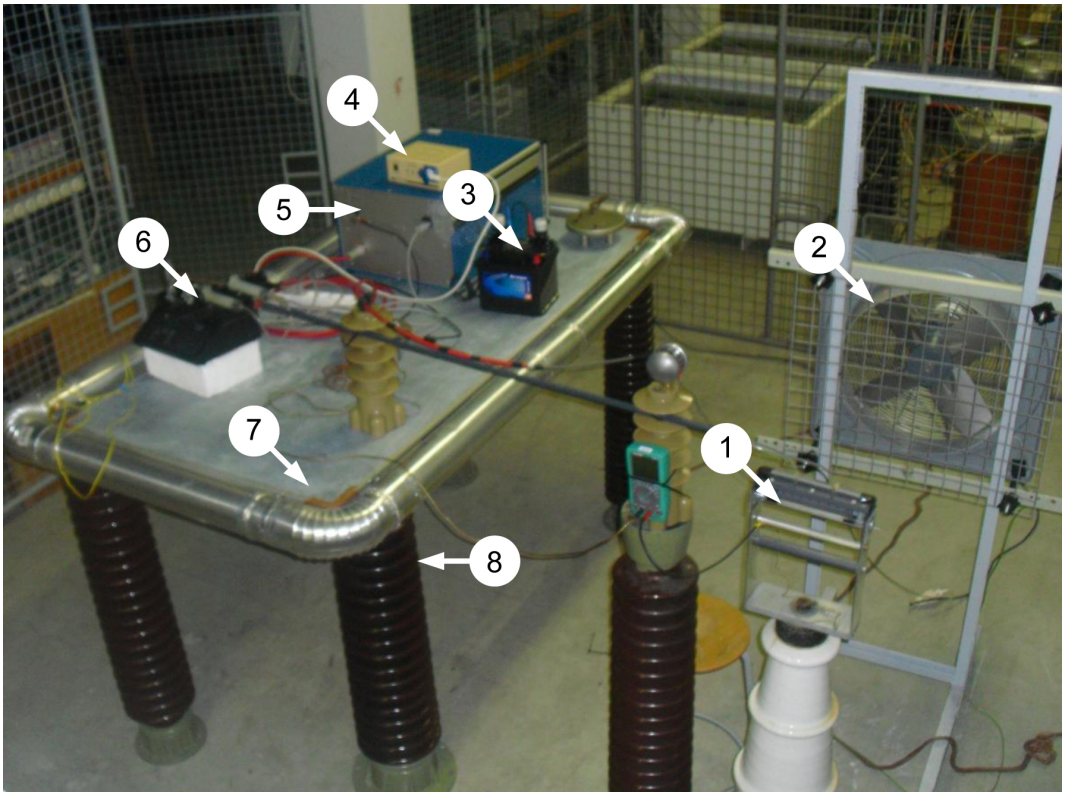

Figure 43: Complete EWICON system. (1) Charging system (2) Wind generator (3) Battery (4) Inverter (5) HVDC source (6) Syringe pump (7) Metal plate acting as a capacitor (8) Ceramic supporting insulator

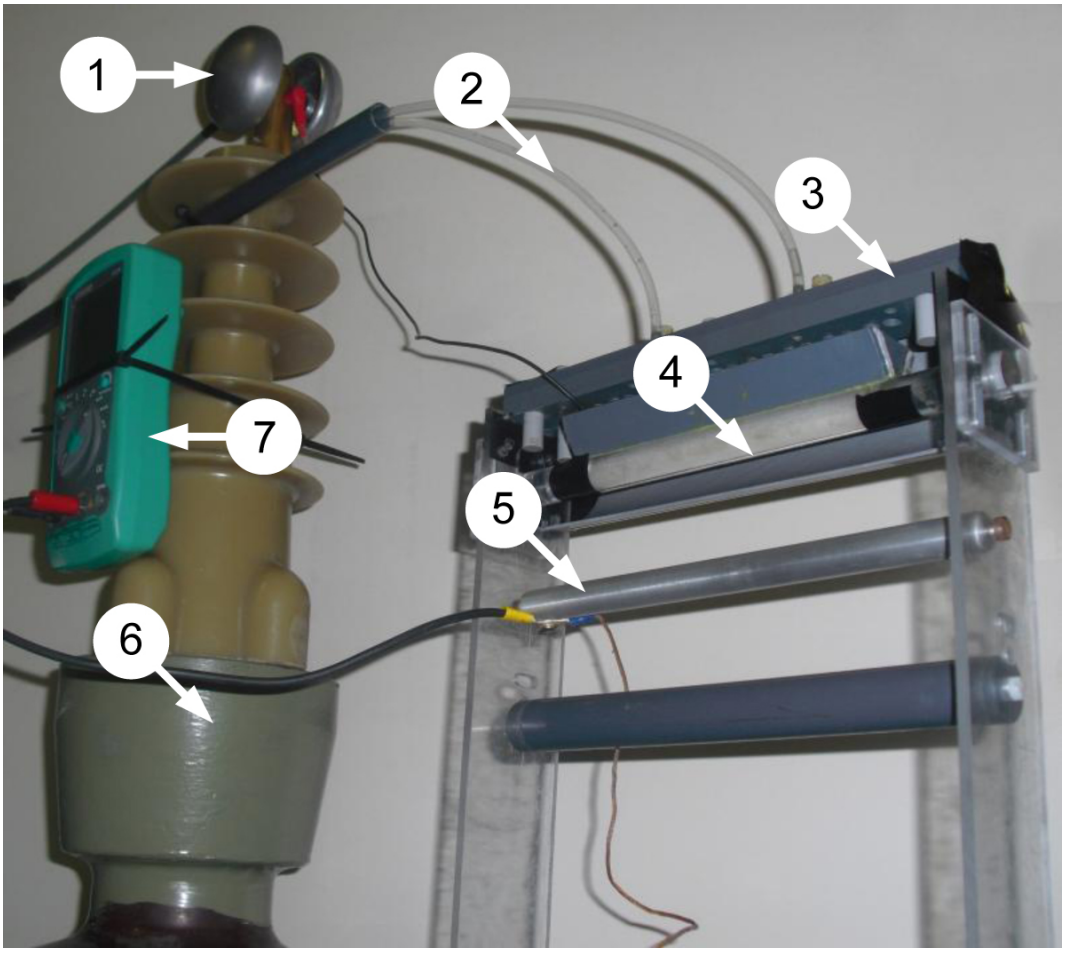

Figure 44: Charging system. (1) High voltage connection (2) Spraying liquid supply (3) Liquid flow dispenser (4) High voltage electrode embedded in porous material (5) Counter electrode (6) Supporting insulator (7) Multimeter to measure current losses.

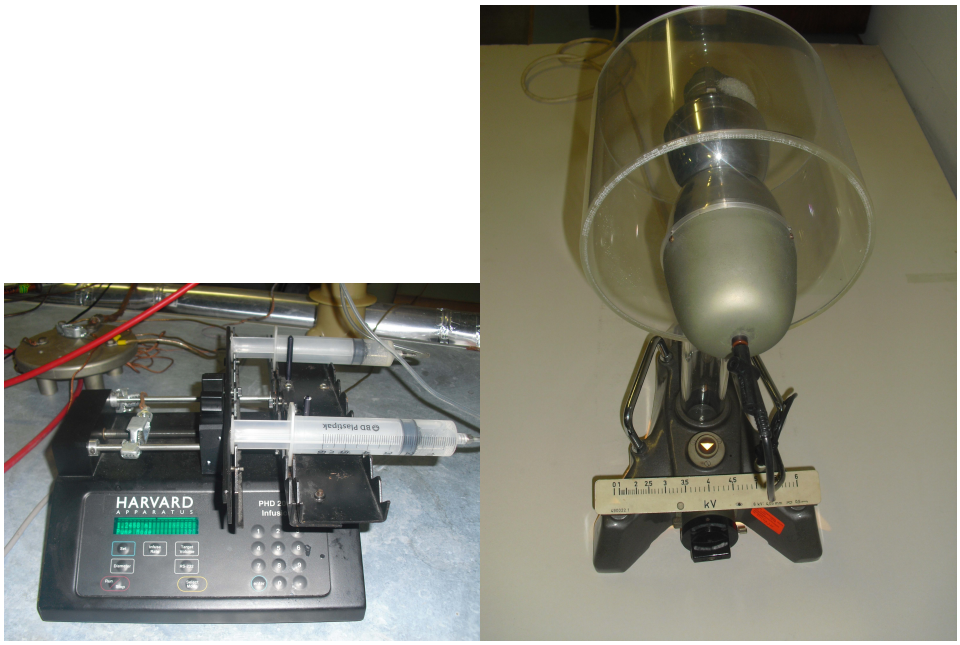

(a) (b)

Figure 45: (a) Syringe pump (b) Electrostatic voltmeter

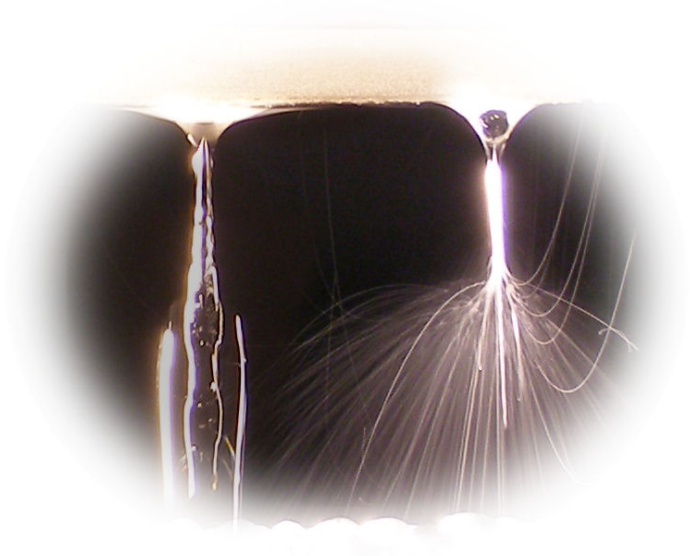

Figure 46: The art of electrospraying

Nomenclature

Symbol	Unit	Description
A	m^2	Area
AH	$g \cdot m^2$	Absolute humidity
C_c	$-$	Correction factor of Cunningham
C_{EWICON}	F	Capacitance of the EWICON
CMR	$C \cdot kg^{-1}$	Charge to mass ratio
d_d	m	Droplet diameter
E	$V \cdot m^{-1}$	Electric field
ε_0	$C^2 \cdot s^2 \cdot kg^{-1} m^{-3}$	Permittivity of vacuum
F	N	Force
γ	$N \cdot m^{-1}$	Surface tension
h	m	Distance between electrodes
η_a	$Pa \cdot s$	Dynamic/Absolute viscosity of air
θ	deg	Cone half angle
I	A	Current
K	$S \cdot m^{-1}$	Conductivity
μ	$Pa \cdot s$	Dynamic/Absolute viscosity
μ_e	$m^2 V^{-1} \cdot s^{-1}$	Electrical mobility
μ_m	$s \cdot kg^{-1}$	Mechanical mobility
P_{max}	W	Maximum recoverable power
P_w	W	Wind power
Q	$m^3 \cdot s^{-1}$	Flow rate
Q_l	$ml \cdot hr^{-1}$	Flow rate used in experiments
q	C	Charge
q_{max}	C	Rayleigh charge limit
R	$-$	Electrode ratio
RH	$-$	Relative humidity
ρ	$kg \cdot m^{-3}$	Density
T	$^\circ C$	Temperature
v_d	$m \cdot s^{-1}$	Droplet velocity
v_T	$m \cdot s^{-1}$	Terminal electrostatic velocity
v_w	$m \cdot s^{-1}$	Wind velocity
V	V	Voltage
V_0	V	Onset voltage
VN	$-$	Viscosity number

Abbreviation	Description
EWICON	Electrostatic wind energy converter
EHDA	Electrohydrodynamic atomization
HPMS	High pressure monodisperse spraying
HV	High voltage
EPI	EWICON perfomance index

References

[1] Key World Energy Statistics 2010, International energy agency (IEA) 2010

[2] Global wind 2009 report, Global wind energy council, 2009

[3] 2009 Renewable Energy Data Book, Energy Efficiency & Renewable Energy, U.S. department of energy, August 2009

[4] Betz A. Das Maximum der theoretisch möglichen Ausnützung des Windes durch Windmotoren. Zeitschrift für das gesamte Turbinenwesen 1920; 26: 307–309

[5] The electrostatic Wind Energy Converter, electrical performance of a high voltage prototype, Dhiradj Djairam, 2008

[6] Electrohydrodynamic atomization in the cone jet mode, from physical modeling to powder production, R.P.A. Hartman 1998

[7] Producing Pharmaceutical Particles via Electrospraying with an Emphasis on Nano and Nano Structured particles - A Review, C.U.Yurteri, R.P.A Hartman, and J.C.M. Marijnissen, Delft University of Technology, 2010

[8] Continued protoype design and testing of self adjusting multinozzle electrospray system using porous technique, Alexandros D. Theodore, 2006

[9] Prototype development of a self adjusting multiple spray EHDA system, Edward McKenna, 2004

[10] The Electrohydrodynamic Atomization of Liquids, David P.H. Smith, IEEE Transactions on industry applications, vol. IA-22, NO. 3, May/June 1986

[11] The production of charged monodisperse fuel droplets by electrical dispersion, A.R. Jones, K.C. Thong, J.Phys. D.Appl. Phys. 1971

[12] Effects of capillary spacing on EDH spraying from an array of cone jets, J.D. Regele, M.J. Papac, M.J.A. Rickard, D. Dunn-Rankin, 2002

[13] Electrosprayed calcium phosphate for biomedical purposes, Sander Cornelis Gerardus Leeuwenburgh, Nijmegen 2006

[14] The production of charged monodisperse fuel droplets by electrical dispersion, A. R. JONES and K. C. THONG, 1971

[15] CRC Handbook of Chemistry and Physics, Internet Version 2005, David R. Lide, ed., <http://www.hbcpnetbase.com>, CRC Press, Boca Raton, FL, 2005

[16] Specific volume and viscosity of ethanol-water mixtures under high pressure, Yoshiyuki Tanaka, Takeshi Yamamoto, Yoshimasa Satomi, Hironobu Kubota, Tadashi Makia, Review of physical chemistry of Japan vol.41 no 1, 1977

[17] Static Dielectric Constants of Water 4- Ethanol and Water + 2-Methyl-2-propanol Mixtures from 0.1 to 300 MPa at 298.15 K, Takashi Moriyoshi, Tetsuro Ishii, Yoshihisa Tamai, and Masafumi Tado, J. Chem. Eng. Data 1990

[18] Koninklijk Nederlands Metereologisch instituut (KNMI)

[19] Perry's Chemical Engineers' Handbook (7th Edition), Perry, R.H.; Green, D.W. 1997 McGraw-Hill

[20] Taylor, G. I. 1964 Disintegration of water drops in an electric eld. Proc. R. Soc. London Ser. A 280 383-397.

[21] Gañán-Calvo, A. M., Davila, J. and Barrero, A. (1997): Current and Droplet Size in the Electrospraying of Liquids. Scaling Laws. J. Aerosol Sci.,28 , pp.249-275

[22] de la Mora, J. F. and Loscertales, I. G. (1994): The Current Emitted by Highly Conducting Taylor Cones, J. Fluid Mechanics, 260, pp.155-184

[23] F.H.Kreuger, Industrial High DC Voltage, Delft University Press, 1995